FUNGAL BIODETERIORATION OF CONCRETE AND ITS PREVENTION USING NANOPARTICLE COATING

A Thesis

Submitted for the partial fulfillment of the continuous assessment of
M.Tech in Environmental Biotechnology course
for the Session 2017-2019

By

SHAHEEN AKHTAR

Roll No. : 001730904007
Registration No. : 141031 of 2017-2018

Under the Guidance of

DR. SUBARNA BHATTACHARYYA

Assistant Professor
Jadavpur University
(School of Environmental Studies)

THESIS (PG/EBT/S/21)

SCHOOL OF ENVIRONMENTAL STUDIES
JADAVPUR UNIVERSITY

2019

যাদবপুর বিশ্ববিদ্যালয়
কলকাতা-৭০০০৩২, ভারত

*JADAVPUR UNIVERSITY
KOLKATA-700 032, INDIA

SCHOOL OF ENVIRONMENTAL STUDIES

It is hereby recommended that this **Thesis** entitled " **FUNGAL BIODETERIORATION OF CONCRETE AND ITS PREVENTION USING NANOPARTICLE COATING** " is prepared and submitted for the partial fulfilment of the continuous assessment of **Masters of Technology (M.Tech) in Environmental Biotechnology** course of Jadavpur University by **Shaheen Akhtar,** a student of the said course for the **session 2017-2019** under my supervision and guidance. It is also declared that no part of this thesis has been presented or published elsewhere.

28/5/19

Dr. Pankaj Kumar Roy

Dean
Faculty of Interdisciplinary Studies,
Law and Management (FISLM)
Jadavpur University

Dean
Faculty of Interdisciplinary Studies, Law & Management
Jadavpur University, Kolkata-700032

28/5/19

Dr. Pankaj Kumar Roy

Director
School of Environmental Studies
Jadavpur University

Director
School of Environmental Studies
JADAVPUR UNIVERSITY
Kolkata - 700 032

Subarna Bhattacharyya

Dr. Subarna Bhattacharyya 28/5/19

(Thesis Supervisor)

Assistant Professor
School of Environmental Studies
Jadavpur University

Subarna Bhattacharyya, Ph.D.
Assistant Professor
School of Environmental Studies
Jadavpur University
Kolkata - 700 032, INDIA

UNIVERSITY OF CALCUTTA

DEPARTMENT OF ENVIRONMENTAL SCIENCE

35, BALLYGUNGE CIRCULAR ROAD, CALCUTTA-700019, INDIA

Punarbasu Chaudhuri, Ph.D.
Assistant Professor

+91 9831140980 (Mobile)
+91 33 2461 5445 Extn. 522 (Off.)
+91 33 25667064 (Res.)
Fax.+91 33 2461 4849
E-mail- *pcenvs@caluniv.ac.in*
punarbasu_c@yahoo.com

It is hereby recommended that this **Thesis** entitled " **FUNGAL BIODETERIORATION OF CONCRETE AND ITS PREVENTION USING NANOPARTICLE COATING** " is prepared and submitted for the partial fulfilment of the continuous assessment of **Masters of Technology (M.Tech) in Environmental Biotechnology** course of Jadavpur University by **Shaheen Akhtar**, a student of the said course for the **session 2017-2019** under my supervision and guidance. It is also declared that no part of this thesis has been presented or published elsewhere.

P.Chaudhuri 28/5/19

Punarbasu Chaudhuri
Assistant Professor
Dept. of Environmental Science
University of Calcutta

Dr. Punarbasu Chaudhuri
Assistant Professor
Department of Environmental Science
University of Calcutta

Date: 28th May, 2019

DECLARATION

This thesis entitled "FUNGAL BIODETERIORATION OF CONCRETE AND ITS PREVENTION USING NANOPARTICLE COATING" is prepared and submitted for the partial fulfillment of the requirements for the award of the degree of Masters of Technology (M.Tech.) in Environmental Biotechnology, course of School of Environmental Studies (Jadavpur University) for the session 2017-2019.

Shaheen Akhtar.

SHAHEEN AKHTAR

Date : 28.05.2019.

School of Environmental Studies,

Jadavpur University.

CERTIFICATE OF APPROVAL

This is to certify that this thesis is hereby approved as an original work, conducted and presented in a manner satisfactory to warrant its acceptance as a pre-requisite to the degree for which it has been submitted. It is implied that by this approval, the undersigned do not necessarily endorse or approve any statement made, opinion expressed or conclusion drawn therein, but approved for the purpose for which it is submitted.

Final Examination for valuation of Thesis

……

……

……

(Signature of the Examiner)

ACKNOWLEDGEMENT

This dissertation work had provided me the opportunity to meet and work with many people whose genuine cooperation and encouragement helped me to successfully complete my work on time. I would thus like to convey my sincere acknowledgement to all those, who in their humble ways had helped me enormously to complete my thesis.

Firstly, my deepest sense of gratitude and special thanks to my thesis supervisor **Dr. Subarna Bhattacharyya**, Assistant Professor, School of Environmental Studies, Jadavpur University, whose constant support, technical advice and valuable guidance lead to the completion of this work. It was indeed an honour and a privilege for me to work under her supervision.

I would like to express my gratefulness to **Dr. Pankaj Kumar Roy**, Director, School of Environmental Studies, Jadavpur University, to provide me the wonderful opportunity and facility to do this dissertation.

I would like to thank **Dr. Tarit Roychowdhury**, Associate Professor, School of Environmental Studies, Jadavpur University, for his continuous encouragement throughout my work.

I would like to convey my sincere gratitude to **Dr. Joydeep Mukherjee,** Associate Professor, School of Environmental Studies, Jadavpur University, for his valuable suggestions and support during my dissertation.

I would also like to thank **Dr. Reshmi Das**, Assistant Professor, School of Environmental Studies, Jadavpur University, for her support and encouragement.

I would like to express my sincere appreciation and gratefulness to **Dr. Punarbasu Chaudhuri**, Assitant Professor, Department of Environmental Science, Ballygunge Science College, University of Calcutta, whose valuable inputs and technical suggestions helped me immensely in my project.

I would like to extend my sincere gratitude towards **Dr. M. Sudarshan,** Scientist F,UGC-DAE, CSR, Kolkata centre for allowing and helping me analyse my samples using Micro XRF facility at his institute.

I would like to thank **Dr. Anupam Ghosh,** Assistant Professor, Department of Geological Sciences, Jadavpur University for allowing and helping me to analyse my samples using Stereo Microscope facility at his department.

I would like to express my sincere acknowledgement to **Dr. Arindam Roy**, Senior Geologist (Paleontology Division), Geological Survey of India (Kolkata Headquarters) for his kind permission and help to analyse my samples using Scanning Electron Microscope (SEM) at their facility.

I would also like to thank **Mr. Samrat Sengupta**, laboratory in-charge/technician, Department of Civil Engineering, Jadavpur University, for allowing me to use his laboratory for the concrete cube preparation and to perform the mechanical tests on my samples.

I would like to show my gratefulness to **Mr. Pankaj Bhadra**, laboratory in-charge/technician, Department of Metallurgical and Material Engineering (School of Material Science and Nanotechnology), Jadavpur University, for helping me in the FTIR analysis of my samples at his facility.

I would like to extend my deepest gratitude to my senior scholar **Anirban Chaudhuri,** whose continuous support, advices and co-operation helped me exceptionally throughout my project.

My sincere thanks to all my senior scholars **Shamayita Banerjee**, **Shouvik Mahanty**, **Utsha Dasgupta, Debolina Chatterjee** and **Dipankar Buragohian.** Without their valuable help my dissertation would not have been a successful one.

I would like to express my appreciation to my fellow batchmates for their cooperation and encouragement.

I would also like to extend my sincere thanks to Mr. Subhasis Ghosh, Mr Manan Das and Mr. Indrajit Saha for their kind cooperation and encouragement.

My Special thanks to Mr. Debasish Maity for his cordial help.

I would also like to thank The School of Environmental Studies, Jadavpur University as a whole for giving me an opportunity to be a part of their family and providing me an excellent workspace.

Lastly, I would like to thank my parents and my brother for always being my source of encouragement and confidence.

Shaheen Akhtar

Kolkata, 2019.

ABSTRACT

This study was aimed primarily to evaluate the fungal biodeterioration of concrete and the effective prevention of this fungal attack on concrete using silicon oxide nanoparticles.

The first part of the work dealt with the optimization of nanosilica coating with a suitable proportion of polyethylene glycol which act as a binder for these nanoparticles thus forming an effective matrix of nanocoating.

In the second part, concrete cubes (dimensions: 7 cm x 7 cm x 7 cm) were prepared and experimented in different set-ups namely control (dry), positive control (moistened), biodeterioration (*Aspergillus tamarii* infected) and prevention (fungus infected nanocoated cubes). Monthly analysis and tests (visual, physical and chemical) were done to evaluate the extension of the biodeterioration in the cubes, for six months. The visual analysis included colour changes, Stereo Microscopy and Scanning Electron Microscopy (SEM) which showed considerable change in the surface deterioration and fungal colonization of biodeteriorated cubes more than the nanocoated concrete cubes. The physical tests included weight loss which showed positive in all the concrete specimens and compressive strength which increased in nanocoated concrete cubes more than that of the biodeteriorated ones. The chemical analysis included pH change in media, Fourier Transform Infrared Spectroscopy (FTIR) and Energy Dispersive X-Ray Fluorescence Spectroscopy (EDXRF) which showed that leaching of calcium ions from the concrete in biodeteriorated cubes were higher than that of nanocoated cubes. Altogether the effectiveness of silicon oxide nanocoating against biodeterioration of *Aspergillus tamarii* was concluded to be positive.

TABLE OF CONTENTS:

LIST OF FIGURES

LIST OF TABLES

CHAPTER I

INTRODUCTION

A large percentage of the world's modern as well as heritage buildings and stone structures have been reported to undergo biological deterioration and attack over time, which ultimately results in the accelerated loss of their unique durable and aesthetic properties. This has turned many heads for the various groundbreaking researches to investigate its causes to a great depth and to introduce feasible applicable techniques to prevent as well as restore these.

Deterioration is a phenomena of down-gradation of materials to a lower vulnerable quality. When this deterioration is brought about by biological factors, it is termed as biodeterioration. It was defined as "any undesirable change in the properties of a material caused by the vital activities of organisms" by Hueck (1965,1968). It is normally perceived to be a negative process. A difference between 'biodegradation' and 'biodeterioration' has been put forward by Allsopp (2004) stating that when microorganisms modify materials with a positive or useful purpose it is referred to as 'biodegradation' and the negative impacts of a microbial activity is referred to as 'biodeterioration.'

Classification of biodeterioration brought about by various microbial community was intensely studied and defined by Allsopp (2004). When material gets damaged due to the direct physical activity such as growth or movement of the microbes, it is known as biophysical biodeterioration. When microorganisms modifies the properties of a material utilizing it as a food and energy source or corrode or pigment the material with their secondary metabolites, it is known as biochemical biodeterioration. When the presence of an organism or its dead body, excreta or metabolic products renders the material's inappropriate appearance, and micro-organisms grows on these otherwise undamaged materials utilizing the surface dirt and detritus it is called soiling. Also the discolouration or aging due to the release of some soluble or insoluble pigments and other metabolites causes fouling. These are sub categorized as aesthetic biodeterioration.

The domain of potential biodeteriogens is quite extensive, starting from macroscopic organisms like fungi, moulds, algae, lichens, insects like termites, carpenter ants, wood boring beetles to microscopic beings like bacteria and cyanobacteria. Biodeterioration caused by bacteria, algae or fungi comprises a significant percentage, in cases of cultural heritage monuments. The severity and irreversibility of these deterioration are quite serious. Colonization of different microorganisms on historic buildings occurs gradually

in a coordinated manner. It is mostly initiated by photolithotrophic algae and cyanobacteria having low nutrient requirements (sunlight, carbon dioxide and sufficient moisture). They secrete lactic, oxalic, succinic, pyruvic and acetic acid thus degrading the stone substrate (Herera et al. 2004, Crispin and Gaylard, 2005). Lichen at times develop on the concrete secreting organic acids releasing carbohydrates and amino acids paved a path for the establishment of heterotrophs (bacteria and fungi). These heterotrophs penetrates the substrate producing organic acids (oxalic, fumaric, citric and 2-ketogluconic acids) and solubilizes the stone components consequently (Warscheid and Braams, 2000). This eventually worsens the physical surface of the substratum, allowing vegetal reproductive plant seeds to be deposited from air (cryptogams spores, weed seeds and higher plant seeds). This ecological succession gets completed when micro-fauna such as red mite *Balaustium murorum, Phaulioppia lucorum* inhabits the substratum (Tiano, 2002).

The mechanism of biodeterioration is influenced by the availability of nutrients and substrates, water permeability, mineral composition, pH, salinity and texture. Numerous environmental factors such as temperature, relative humidity (RH), and light conditions also influences the microorganism's growth on the substratum (Rajkwoska et al., 2013).

Fungi being multicellular, heterotrophic organisms are considered to be the most established detrimental microbes (Biswas et al., 2013) and can be found extensively in all sorts of environments. They can be seen thriving naturally on various stone works and wooden structures and can effectively withstand dry conditions. The growth of black meristematic fungi which includes genera of *Alternaria, Aspergillus* and *Cladosporium* have resulted in surface erosion and micro-fractures in the Milan Cathedral of Italy (Capitelli et al., 2017). Genera like *Botrytis, Mucor* and *Trichoderma* produces citric and oxalic acid that solubilizes silicates and thus results in weathering of stones (Gorbushina et al., 2000). Water damaged and damp buildings are a breeding ground for moulds and fungus especially *Penicillium chrysogenum* and *Aspergillus versicolor* which are most common in water-damaged buildings, and *Chaetomium* spp., *Acremonium* spp., and *Ulocladium* spp being common in damp buildings (Andersen et al., 2011).

The main focus for the study of biodeterioration of materials is the establishment of various prevention, control and restoration techniques against it. Ultra violet (UV) rays has a germicidal activity on algae, bacteria and fungi with being highly effective during their logarithmic phase of growth at low relative humidity (50%-60%).Though its

penetration power is low, it can modify the components such as proteins or cellulose of certain substrates (Tiano, 2002). Electromagnetic radiation such as gamma rays have been proved to be very much effective against moulds and insects developed on paper, parchment and wood (Hickin, 1971). A biological agent such as the fungus *Scytalidium lignicola* can suppress the growth of *Lentinus lepideus*, which is a wood-decaying fungus. The former is commercially used and is hostile towards the growth of the latter biodeteriogen on archaeological wood (Bruce, 1998). Oxidizing agents like bromide, chloramine, ozone, aldehydes like formaldehyde, glutaraldehyde and esters of hydroxybenzoic acid (parabens) are all potential biocides. Isothiazolinones are also considered to be effective biocides. The methyl (MIT) and benzyl (BIT) derivatives are potent bacteriocides whereas the octyl (OIT) and the dichloro-octyl (DCOIT) derivatives show productive antialgal and antifungal activity (Allsopp, 2004). A study conducted by Osman et al., (2018) evaluated the inhibitory effects of various concentrations of dimethyl sulfoxide (DMSO) on fungus growing on archaeological wood. Commercial products like Panacide, Linquad and Preventol PN (a solid preparation of tebuconazole and triadimefon) are effective against high fungal stains on mural paintings of Casas Pintadas of Évora, Portugal (Rosado et al., 2017).

Particles having dimensions within 1-100 nm range (nanoparticles) has unusual advantageous properties over their bulk counterparts. Thus their use in the restoration process is a new inclusion. Titanium dioxide (TiO2) nanoparticles are photocatalytic materials that can catalyze the complete degradation of many organic contaminants and has thus been used for protecting marble facades of historic buildings (Aldoasri et al., 2017). TiO2 nanoparticles thus opposes degrading process due to biological attacks, stains or attacks by NOx and SOx. Silver (Ag) nanoparticles and titanium oxide (TiO2) nanoparticles based nanocomposite treatment of limestone in the Cathedral of Seville (Spain) showed effective biocidal effect (Becerra et al., 2018). Consolidants made from nanoparticles or nanocomposites of silicon (Si), titanium (Ti), silver (Ag), cadmium (Cd), iron (Fe), zinc (Zn) and cobalt (Co) have proved to be effective in the conservation of cultural heritage monuments and buildings (Fernandez et al., 2016).

Fungal attack on building materials especially concrete and their different prevention methods has been an interesting and ongoing topic for various research works in the last decade and has produced many convenient results. The incorporation of nanoparticles

for better construction purposes and in admixtures, is probably a more recent addition to the numerous techniques developed for preventing microbial biodeterioration.

The data generated from the present study may prove helpful for the assessment of biodeterioration by common fungal species on concrete and its effective and non-destructive prevention using easily available nanoparticles.

CHAPTER II

AIMS & OBJECTIVES

The prime aim of this present dissertation work is to determine the fungal biodeterioration of concrete by *Aspergillus tamarii* and its effective prevention with the application of silicon oxide nanoparticles.

The study was carried out with the following objectives:

- To evaluate the microbial deterioration effect on concrete caused by the infection of fungal species (*Aspergillus tamarii*).
- To optimize the ratio of nanosilica to be used in the study.
- To evaluate the effectiveness of the applied nanocoating with respect to the prevention of concrete biodeterioration.
- To interpret the biodeterioration effect and the feasibility of the nanocoating prevention on concrete using standard tests and analysis.

Scope of study :

- ✓ Preliminary laboratory study of the aforementioned proposed model on concrete pieces.
- ✓ Optimization of the nanocoating that is to be used.
- ✓ Preparation of concrete cubes of dimension 7 cm x 7 cm x 7 cm for the biodeterioration and prevention tests.
- ✓ Monthly assessment of the concrete specimens for six months, for pH, colour change, weight loss, compressive strength test, Stereo microscope imaging, Scanning Electron Microscope (SEM) imaging, Energy Dispersive X-Ray Fluorescence (EDXRF) spectroscopy and Fourier Transform Infrared (FTIR) spectroscopy analysis.

CHAPTER III

LITERATURE REVIEW

3.1 Fungal Biodeterioration of Concrete : Review of Literature

Shelter is one of man's basic necessities, the dwelling place of a man i.e. buildings are thus needed to be protected from biodeterioration for the well-being of their own kind. On the other hand, heritage monuments and structures represents the roots of our culture and are too required to be preserved as well as restored from microbial attacks. Biodeterioration is thus a major cause in affecting buildings and monumental structures adversely.

One of the most commonly used material for construction purposes and being a $100 billion dollar industry, concrete is a structural material which is a composite of fine and coarse aggregates bonded together with the help of cement and water. The usage of concrete-like materials can be dated back to 6500 BC by the Nabataea traders or Bedouins inhabiting the Arabian Peninsula, North Africa, Iraq and the Levant. It was also extensively used in the later Eras of Ancient Egyptians, Romans and Greeks. Today, with time, the application and usage of concrete has drastically increased.

Concrete is made up of three major ingredients, aggregate that includes both fine and coarse materials like sand, gravel and crushed stones which helps in increasing the strength of the concrete, cement that is composed of alumina (2.5%-6%), silica (19%-23%), lime (61%-67%), iron (0%-6%) and gypsum (1.5%-4.5%) and water that allows the cement to move freely (slurry like).Cement hardens when mixed with water and binds all the ingredients together. Portland cement is the most widely used cement at present times. Stronger, more durable concrete should have a lower water-to-cement ratio. The property of the final product depends on the ratio of these ingredients. Admixtures are often added to adjust the concrete mixture for specific performance. Strength, durability, versatility and affordability are the properties that makes concrete the most preferable building material.

Building materials especially concrete exposed to fungal activities are prone to drastic physical, chemical, mineralogical and microstructural irreversible damages through the biochemical processes that the microbial species utilizes to react, develop and proliferate (Bertron 2015).

Fungus has a capability to do so with their developing hyphae that etches into the interior of the concrete. This was proved by the study done by Gu et al., (1998) showing that with the fungal proliferation of *Fusarium* on concrete for 120 days, organic acids were excreted that resulted in the dissolution of the available calcium and magnesium ions in the concrete. Dissolution of these ions lowered the pH of concrete which resulted in an unstable state of the binding paste and hence gets more prone to mechanical weathering (Mehta et al., 1999) and cracks can easily develop in them (Gu et al., 1998). This adversely affected the porosity of the concrete by increasing it and enlarging the damaged area. Because of this the weight and compressive strength of the concrete also got affected (Gu et al., 1998).

A study conducted by Biswas et al., 2012 stated that pre-historic caves in Kabra-Pahad (Chattisgarh) were found to have undergone destructive microbial deterioration. When the microbe organisms were isolated from the affected regions of the natural structure, it was found that *Aspergiilis sp.* was the most predominant one among all the other isolated species.

Biogenic weathering effects of fungal species: *Aspergillus niger*, *Serpula himantioides* and *Trametes versicolor* on apatite, galena and obsidian minerals by Adeyemi et al.,(2005) using EDXRF and SEM micrographs showed that the interactions of metabolites like H^+ and organic acids exuded by these fungus were the primary responsible force for the modification of the mineral substrates of the rocks into the transformation of secondary minerals or crystals and subsequently leading to the corrosion of the mineral surface.

Wei et al., (2013) observed that microbial colonization, succession and its induced deterioration through organic and inorganic acid production, caused corrosion in concrete sewer lines and structures and also compromised with its structural integrity which is a significant problem worldwide.

3.2 Prevention of Fungal attack using Silicon oxide Nanoparticles : Review of Literature

Nanotechnology is the newest trend of most of the scientific researches and developments that are taking place in this century. Nano-sized particles exists at near atomic levels and can be enhanced to cater mankind's needs appropriately.

Silicon dioxide is the main component of beach sand as silica is the second most abundant element found on Earth's surface. Silicon dioxide nanoparticles (also called silica nanoparticles or nanosilica) have properties of stability and ability to be functionalized with a wide range of molecules and polymers. The P-type nanosilica particles have higher surface area than S-type nanosilica particles, having a pore rate of 0.061 ml/g and flaunts higher ultraviolet reflectivity. Commercially available SiO_2 NPs with average particle size of 7 -14 nm and a specific surface area of 100-150 m^2/g exhibits prominent hydrophobicity.

Alcohol suspension of SiO_2 NPs when sprayed onto a paper by Ogihara et al., (2012*),* formed a transparent coating and imparted superhydrophobicity to the paper. The hydrophobic character of SiO_2 NPs can be enhanced by the incorporation of hybrid siloxanes or silicone polymers which presented a high water repellant capacity generating superhydrophobicity. Superhydrophobic surfaces displays a wetting characteristics with a very high static contact angles (water contact angle with the surface) which can be greater than 150°. Mixing alkoxysilane and silica nanoparticles synthesized by sol-gel route using HCl as a catalyst and ethanol as a solvent, De Ferri et al.(2011) obtained a superhydrophobic product for stoneworks.

Studies conducted by Falchi et al.(2013) showed that application of commercial nanosilica with an average radius of 9-55 nm, on limestone (Lecce stone) has proved to be a strong consolidant. The pre-treatment of the surface with ethanol and the nanoscale size of the silica particles resulted for a better consolidation action. Surfactant-synthesized silicon-based hybrid nanocomposites such as tetraethoxysilane (TEOS) and methyltrimethoxysilane (MTMOS) are among the most widely used stone consolidants due to their ability to penetrate easily into porous matrix (Wheeler et al. 2005). The addition of small amount of surfactant like n-octylamine during the nanocomposite preparation gives crack-free consolidants for stone conservation (Mosquera et al., 2012).

These silica-based consolidants can hence be considered fairly compatible with silicate stones.

SiO_2 NPs expresses good inhibitory property of different bacterial strains. Their smaller size and higher surface to volume ratio enables them to bind with the microbial strains and thus contributed to their antimicrobial potential. A study by Farrukh et al.(2016) showed that ZnO-SiO_2 nanocomposite exhibited antibacterial activity against *Bacillus subtilis* (gram positive) and *Escherichia coli* (gram negative) strains and antifungal activity against *Candida parapsilosis* and *Aspergillus niger*. SiO_2 in the nanocomposite was also observed to enhance the photo-catalytic activity of the nanocomposite.

In another research conducted by Scevola et al.,(2012*)* a product named SIAB was synthesized which consisted of stable nanosilica functionalized with ionic Silver. The antimicrobial property of SiO_2 NPs were observed to be improved by the covalent bonding of the Ag ions, stabilized in their one electron oxidized form. The activity of SIAB was tested against various different gram-positive and gram-negative bacteria and fungi. *Staphylococcus aureus*, *Enterococcus* spp., *Streptococcus pyogenes*, *Streptococcus salivarius*, *Streptococcus mitis*, *Pseudomonas aeruginosa*, *Escherichia coli* and *Candida albicans*. It was concluded from the study that SIAB showed high bacterial and high fungicidal action against these strains.

The replacement of cement with nanosilica having an average particle size of 15 nm and 80 nm showed an increase in compressive strength of the nanosilica blended concrete. An increase in flexural and split tensile strength as well was observed in blended concrete with 80 nm nanosilica (Givi et al., 2010).

In another study conducted by Li et al., (2004) showed that nano Fe_2O_3 and nano silica mortars exhibited higher 7 days and 28 days compressive strength than normal concrete. The analysis of the microstructure showed that due to pozzolanic reaction, nanoparticles filled up the pores and substituted the reduced calcium hydroxide amount.

The incorporation of nanosilica can improve the microstructure to be more uniform and compact as compared to normal concrete thus enhancing the resistivity of concrete to water (Ji, 2005).

CHAPTER IV

METHODOLOGY

4.1 Preparation of Fungal Spore Suspension :

4.1.1 Pure Culture Preparation :

Pure culture of *Aspergillus tamarii* were prepared in Czapek Dox agar slants initially. 50 ml of Czapek Dox media was prepared in four 100 ml conical flasks as per the following Czapek Dox Composition : (HiMedia Technical Data)

Ingredients	**Amount (gms/litre)**
Sucrose	30
Sodium nitrate	2
Dipotassium phosphate	1
Magnesium sulphate	0.5
Potassium chloride	0.5
Ferrous sulphate	0.01
Agar	15
Final pH (at 25°C)	7.3±2

The ingredients were mixed, pH was adjusted, after adding the agar the media was autoclaved at 121°C temperature at 15 pounds per square inch (1.0546 Kg/cm^2) pressure for 30 minutes. 200 ml of distilled water was also autoclaved. After the sterilization of Czapek Dox media, it was cooled and kept at an angle of 45° overnight for solidifying, at room temperature. After solidification, the agar slants were streaked with a loopful (inoculating loop) of pure culture of *Aspergillus tamarii* and then incubated at their optimum growth temperature of 29°C for 7 days.

Figure 1: (i) Streaked agar slants before incubation (ii) Pure slants of *Aspergillus tamarii* after incubation of 7 days.

4.1.2 Spore Suspension Preparation :

On completing the incubation period of 7 days, the slants were taken out of the incubator and 50 ml of autoclaved (sterile) distilled water was added to each flasks. The flasks were shaken properly so that the spores from the pure culture gets suspended into the added sterile distilled water. The total 200 ml of spore suspension (50 ml from each of the 4 flasks) was thus collected in a fresh autoclaved conical flask and was stored for further use.

4.2 Nanoparticle Coating Optimization and Preparation:

Silicon oxide nanoparticles were commercially obtained (Platonic Nanotech Private Limited) having the following specifications:

Chemical Formula	**:**	SiO_2
Physical Form	**:**	Powder
Colour	**:**	White
Purity	**:**	99.55%
Average Particle Size	**:**	30-50 nm
Specific Surface Area	**:**	200-250 m^2/g
Atomic Weight	**:**	231.533 g/mol
Bulk Density	**:**	0.10 g/cm^3
True Density	**:**	2.5 g/cm^3
Morphology	**:**	Porous
Molar Mass	**:**	60.08 g/mol
Melting Point	**:**	1600 °C

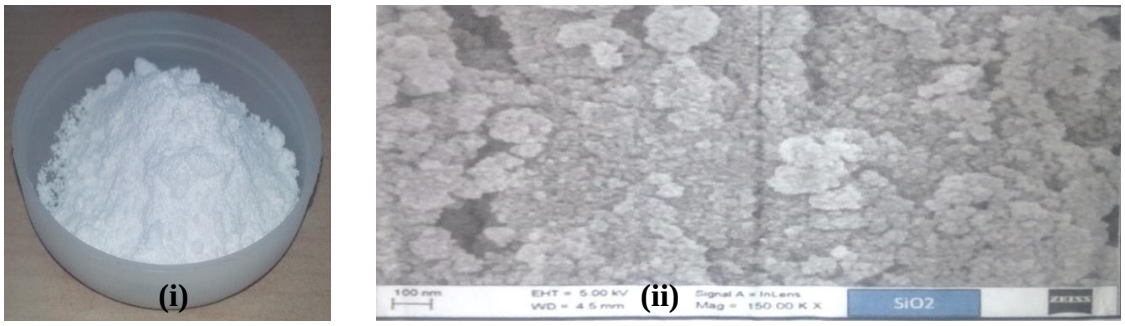

Figure 2: (i) commercially obtained white Nanopowder of SiO_2. (ii) Scanning Electron Microscopic (SEM) image of the SiO_2 nanoparticles with an average particle size of 30-50 nm (provided by Platonic Nanotech Private Limited).

4.2.1 Binder Preparation :

Polyethylene glycol (PEG) was dissolved in ethanol [1:1 ratio] by gently heating in a water bath at 35°C for 20 minutes. The PEG flakes dissolved to give a thick, translucent and fairly viscous solution.

4.2.2 Optimization of Nanoparticle Coating :

At first, for the optimization of the ratio of the nanoparticle coating, 4 combinations of binder, silicon oxide nanopowder and water were tested. The combinations being:

Binder (ml) : Silicon oxide nanopowder (g) : Distilled water (ml)

1) 1 : 0.1 : 2
2) 1 : 0.5 : 2
3) 1 : 1 : 2
4) 1 : 5 : 2

Milky white solutions of the above 4 combinations were prepared, sonicated for 5 minutes and then spread on glass petri plates uniformly. The petri plates were then kept in the hot oven dryer at 40°C for 2 days. After 48 hours of drying, the petri plates were taken out and the nanocoats in each petri plate was observed. The 3rd and 4th combination nanocoating were found to be thick and brittle. The 1st combination nanocoating did not adhere properly to the petri plate surface. The 2nd combination nanocoating formed almost a perfect film on the petri plate surface.

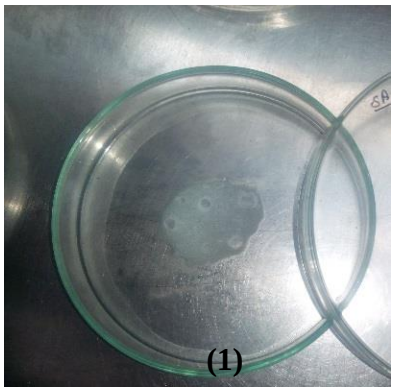

(1)

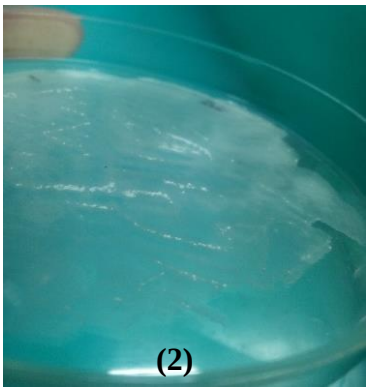

(2)

Figure 3: The 4 combinations of binder, silicon oxide nanopowder and distilled water after 48 hours of drying (1) Ratio-1 : 0.1 : 2 (2) Ratio-1 : 0.5 : 2 (3) Ratio-1 : 1 : 2 (4) Ratio-1 : 5 : 2.

Thus, the 2nd combination of binder, silicon oxide nanopowder and water (1 : 0.5 : 2) was chosen to be proceeded further in the study.

4.2.3 Preparation of Nanoparticle Coating :

Figure 4: The aqueous milky white coloured Nanoparticle coating after the mixing of the binder, nanopowder and water.

For the study; 25 ml binder, 12.5 g Silicon oxide nanopowder and 50 ml distilled water were mixed and sonicated for 5 minutes (avoiding froth formation on the surface) at room temperature. A milky white homogenous solution of nanoparticle coating was obtained.

4.3 Preliminary Laboratory Study :

4.3.1 Fungal Biodeterioration of Concrete Pieces (First 3 months study) :

18 concrete pieces were hammered to approximately same size and their initial weights were measured. Six 250 ml sterile conical flasks were taken and the concrete pieces were distributed in those (3 pieces in each flask). 150 ml of Czapek Dox media was prepared and autoclaved along with 150 ml of distilled water. The media and the autoclaved water was then cooled down to room temperature and distributed in the conical flasks (50 ml media each in 3 flasks marked for biodeterioration study and 50 ml autoclaved water each in 3 other flasks marked for control). 5 ml of fungal spore suspension was added to the three flasks that were marked for biodeterioration study of the concrete pieces (spore suspension to media ratio being 1:10).

Thus the arrangement was as follows:

Control ➞ 3 conical flasks ➞ Concrete pieces + Autoclaved distilled water

Biodeterioration ➞ 3 conical flasks ➞ Concrete pieces + Czapek Dox media + Fungal spore suspension

The conical flasks were cotton plugged, the control setup was kept at room temperature and the biodeterioration setup was placed in the incubator at 29°C for 3 months. At the end of every month, a flask was removed from each setup to record the colour change and the weight loss percentage of the respective concrete pieces.

4.3.2 Fungal Biodeterioration of Concrete Pieces and its Prevention with Nanocoating (Second 3 months study) :

27 concrete pieces were hammered to approximately same size and their initial weights were measured. 9 concrete pieces were taken and brushed uniformly with previously prepared silicon oxide nanocoating. The nanocoated concrete pieces were dried in the hot oven dryer for 4 days at a temperature of 40°C. All the concrete pieces were then distributed in nine 250 ml sterile conical flasks equally (3 concrete pieces in each conical flask). 300 ml Czapek Dox media was also prepared, autoclaved, cooled and distributed

in six conical flasks (50 ml media in each flask). 5 ml of fungal spore suspension was then added to these six flasks (spore suspension to media ratio being 1:10).

Thus the arrangement was as follows:

Control	➞	3 conical flasks	➞	Concrete pieces only
Biodeterioration	➞	3 conical flasks	➞	Concrete pieces + Czapek Dox media + Fungal spore suspension
Nanoparticle coated	➞	3 conical flasks	➞	Nanocoated concrete pieces + Czapek Dox media + Fungal spore suspension

The conical flasks were cotton plugged and kept in the incubator at 29°C for 3 months. At the end of every month, a conical flask was removed from each setup to record the colour change and the weight loss percentage of the respective concrete pieces.

4.4 Study of Fungal Biodeterioration of Concrete Cubes and its Prevention using Nanoparticle coating:

4.4.1 Preparation and making of Concrete cubes :

Concrete cubes of standard grade M20 (final compressive strength after 28 days of curing :20 Mpa or 20 N/mm^2) were made as follows :

As per design standard of grade M20, cement, sand (fine aggregate) and stone chips (coarse aggregate) were weighed according to the ratio of 1:1.5:3. Firstly, the sand and cement were mixed thoroughly in dry condition using a shovel to achieve a uniform colour. Then the stone chips were added and the entire batch were mixed uniformly. Water was then added to this mixture (water to cement ratio being 0.6) and all the components were homogenously mixed to obtain the desired consistency.

Cubic cast iron moulds were cleaned and oiled and the freshly mixed concrete was then immediately filled up in the moulds, layer by layer, followed by uniform compaction using a compacting bar to eliminate any void. The moulds were completely filled and the top surface was leveled by a trawler. The moulds were then kept at room temperature for 24 hours.

After 24 hours, the moulds were removed and solid concrete cubes of dimension 7 cm x 7 cm x 7 cm were obtained. These cubes were then submerged in clean water for 28 days for curing. Having gained the maximum strength, the cubes were taken out of water and dried for 3 days at room temperature. The initial weights of the cubes were recorded in a weight balance followed by the measurement of their initial compressive strength.

Figure 5: Concrete Cubes preparation : (a)Cement, sand and stone chips mixed in a ratio of 1: 1.5 :3 (b)Water added to obtain the concrete mix (c)Cubic cast iron moulds (d)Concrete poured and leveled in cast iron moulds (e)After drying overnight (f)Cubes submerged in water for curing of 28 days (g)Concrete cubes after curing and 3 days of drying.

4.4.2 Nanocoating the cubes :

The cubes that were selected for the study of prevention of fungal biodeterioration were brushed uniformly with the previously prepared Silicon oxide nanocoating. These cubes were then kept in the hot oven dryer at 40°C and were dried for 4 days.

Figure 6: Nanoparticle coated Concrete Cubes in hot air oven after 4 days of drying at 40°C.

4.4.3 Media Preparation :

4 L of Czapek dox Media was prepared and its pH was adjusted to 7.3±2. It was then autoclaved for 40 minutes and cooled down to room temperature.

Figure 7: Prepared Czapek-Dox Media (broth).

4.4.4 Preparing the experimental setups :

Polyethylene boxes were surface sterilized with ethanol followed by UV radiation treatment for 1 hour. Non-reactive sterilized plastic scrubbers were placed at the bottom of the boxes marked to study the biodeterioration and the prevention process, along with the addition of 2 L of Czapek Dox media and 200 ml of fungal spore suspension to each of these boxes. The cubes were distributed in all the boxes and were tightly sealed.

The arrangement was as follows:

Set-up		Contents
Control	➞	Box + Concrete cubes
Positive Control	➞	Box + Moistened Concrete cubes
Biodeterioration	➞	Box + Scrubber + Czapek Dox media + Fungal inoculation + Concrete cubes
Prevention	➞	Box + Scrubber + Czapek Dox media + Fungal inoculation + Nanocoated Concrete cubes

The cubes of positive control were sprinkled with water every month whereas the cubes of control were kept dry throughout the study.

This experimental setup was kept at room temperature for 6 months and after every month, cubes from each set were removed and tested to observe the changes.

Figure 8: (i)Control set-up (ii)Positive Control set-up (iii)Biodeterioration set-up (iv)Prevention set-up (v)The Final Experimental Set-up arrangement.

4.5 Tests and Analysis done on the Concrete cubes :

4.5.1 Humidity measurement :

At the end of each month, the humidity inside the boxes marked for positive control, biodeterioration and prevention were recorded using a digital humidity meter.

Figure 9: Digital Humidity meter (Lutron).

4.5.2 pH measurement :

After every month, the pH of the media at the bottom of the boxes in biodeterioration set-up and the prevention set-up, and the pH of the surface of moistened concrete cubes contained in these boxes, were checked and noted down using a pH indicator paper (Merck).

4.5.3 Colour change observation :

At the end of every month (6 months in total), concrete cubes from each of the experimental set-up (3 cubes each from control, positive control, biodeterioration and prevention set-ups respectively) were taken out, thoroughly cleaned and then dried in hot air oven for 6 hours at a temperature of 80±5 °C. These cubes were then kept in a desiccator for 4 hours.

The concrete cubes were then observed by naked eye and simultaneously compared to a geological rock colour chart (Munsell, 2003), for any colour change.

4.5.4 Weight loss measurement :

After the concrete cubes were prepared and dried properly, initial weights of each concrete cube was measured in a weighing machine. The cleaned, dried and desiccated concrete cubes taken out at the end of each month from the respective experimental set-ups, were weighed in the weighing balance to record their final weights.

Figure 10: The weight of a concrete cube being measured in the weight balance.

From the weights measured, the percentage weight loss of the concrete cubes were calculated using the formula:

$$\text{Change in weight (kg)} = (W_1 - W_2) / W_1$$

Where, W_1 = Initial weight of the concrete cube (kg)

W_2 = Final weight of the concrete cube (kg)

So, Percentage weight loss (%) = change in weight x 100

4.5.5 Stereo Microscope :

A stereo-microscope is an optical microscope having a low magnification with a longer working distance. It primarily uses two separate optical paths using two separate objectives and eye pieces for each eye thus yielding a three-dimensional visualization of the specimen. It also uses reflected illumination of the specimen i.e. it utilizes the light that is naturally reflected from the object rather than transmitted through it. These features altogether makes it ideal for examining solid material's surfaces, circuit board inspection, watch making and also to be used in dissection, microsurgery, and in forensic engineering.

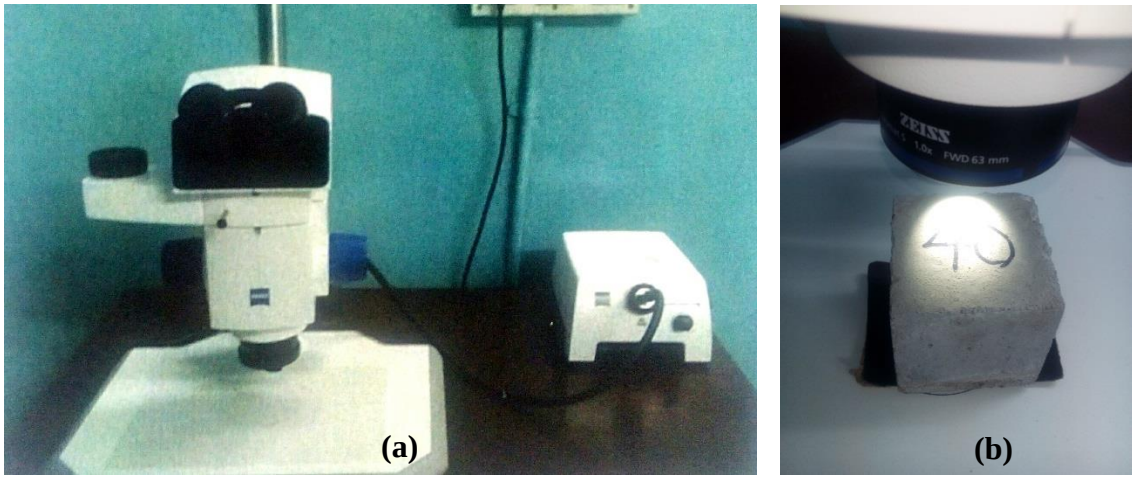

Figure 11: (a) Stereo Microscope (Discovery,V8) (b) Concrete cube observed under the stereo microscope.

The concrete cubes that were taken out every month from all the 4 set-ups (for 6 months) were observed under the stereo microscope to note any change on their infected surface.

4.5.6 Compressive Strength test :

Compressive strength is the maximum stress that a solid material can sustain without fracture, under a gradually applied load tending to reduce size. Determining the compressive strength of concrete is the most common performance measurement and a key value for designing structures.

The compressive strength of the cubes were determined using a Universal Compressive Strength Test Machine. Each concrete cube specimen was placed between the platens

such that the load could be applied on opposite sides of the cubes, and the axis of the specimen and the centre of thrust of the spherically seated platen are vertically aligned. Load was applied to the specimen at an increasing rate of 140 kg/cm^3 per minute till the specimen collapsed. The peak load or the maximum applied load at which the cube failed was noted and the corresponding compressive strength was calculated as follows:

$$\text{Compressive Strength of Concrete (N/mm}^2\text{)} = \frac{\text{Maximum Load applied to the cube}}{\text{Cross-sectional Area of the cube}}$$

Figure 12: (i) and (ii) :Universal Compressive Strength Test Machine (iii) Concrete cube placed between the spherical plattens for strength test.

During the compressive strength test, all the concrete cubes were found to be collapsed and broken. Small pieces of concrete were then collected from these broken cubes to be further tested and analyzed in various other sophisticated instruments.

4.5.7 Scanning Electron Microscope (SEM) :

A scanning electron microscope utilizes a focused electron beam over a specimen surface to create an image whose resolution is superior to that of a light microscope. At the surface of the specimen, these high-energy electrons generates a variety of signals that provides information about the specimen topography, external morphology and texture. Its capability of analysis of selected point locations of the specimen proves useful in quantitative or semi-quantitative determination of the specimen's chemical compositions, crystalline structure and crystal orientation.

Figure 13: Scanning Electron Microscope (SEM).

The small concrete pieces that were collected from the broken cubes after the strength test, were carbon coated, dried for a few hours and then viewed under the scanning electron microscope.

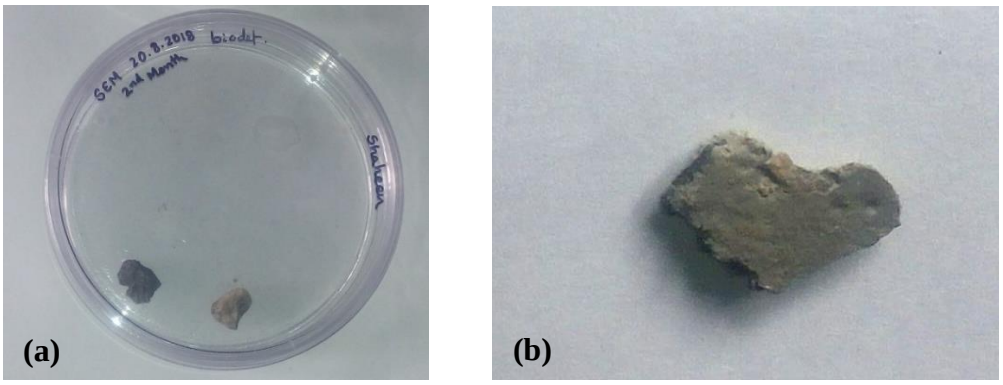

Figure 14: (a) Concrete pieces that were used for SEM analysis (b) Carbon coated Concrete piece.

4.5.8 Fourier Transform Infrared Spectroscopy (FT-IR) :

Fourier Transform Infrared Spectroscopy is an analytical technique that identifies the organic, polymeric and sometimes inorganic components of a sample using infrared absorption or emission of the solid, liquid or gaseous sample, over a wide spectral range. The basic principle of FT-IR is by shining a beam of light, containing many frequencies, on the sample resulting in the production of an interferogram of sample signals. The FT-

IR then collects these interferogram of signals using an interferometer, digitizes and performs a Fourier Transform (FT) function on the interferogram and displays the spectrum.

Spectral quality determination is an important step in the spectrum interpretation process. General classification of materials by its major functional groups can be done with a good quality spectrum whereas a poor quality spectrum can misrepresent the true absorption band positions, shapes and intensities.

One of the popular interpretation of the resultant spectra is through spectral fingerprinting where the spectrum of the unknown sample is compared to the known molecular configurations, in order to determine the structure of the unknown sample. The spectrum is divided into several frequency regions and the presence or absence of absorption bands in each region interprets the sample characteristics.

Figure 15: Fourier Transform Infrared Spectrometer (FT-IR).

The small pieces of concrete that were earlier collected after the compressive strength test, were uniformly crushed using a mortar and a pestle, and the corresponding homogenous powder of concrete was used in FT-IR spectroscopy analysis.

4.5.9 Energy Dispersive X-Ray Fluorescence Spectroscopy (EDXRF) :

Energy Dispersive X-Ray Fluorescence spectroscopy is a highly accurate, non-destructive technique for the elemental analysis (both qualitative and quantitative) of an unknown sample. The complete breakdown of the composition to elemental level, of known as well as unknown materials in terms of percentages or ppm (parts per million) is easily obtainable. In EDXRF spectrometers, concurrent excitation of all the elements in a sample are done which emits a fluorescence radiation. This fluorescence radiation from the sample is collected using an energy dispersive detector along with a multi-channel analyzer which simultaneously separate the different energies of the characteristic radiation from each of the different constituent elements of the sample.

Figure 16: Energy Dispersive X-Ray Fluorescence (EDXRF) Spectrometer (Horiba Scientific, XGT-7200).

The powdered samples of concrete, obtained from crushing of the small concrete pieces using mortar and pestle, were analysed in the EDXRF spectrometer.

CHAPTER V

RESULTS & DISCUSSIONS

5.1 Preliminary laboratory study :

5.1.1 Fungal Biodeterioration of Concrete Pieces (First 3 months study) :

5.1.1.1 Colour change :

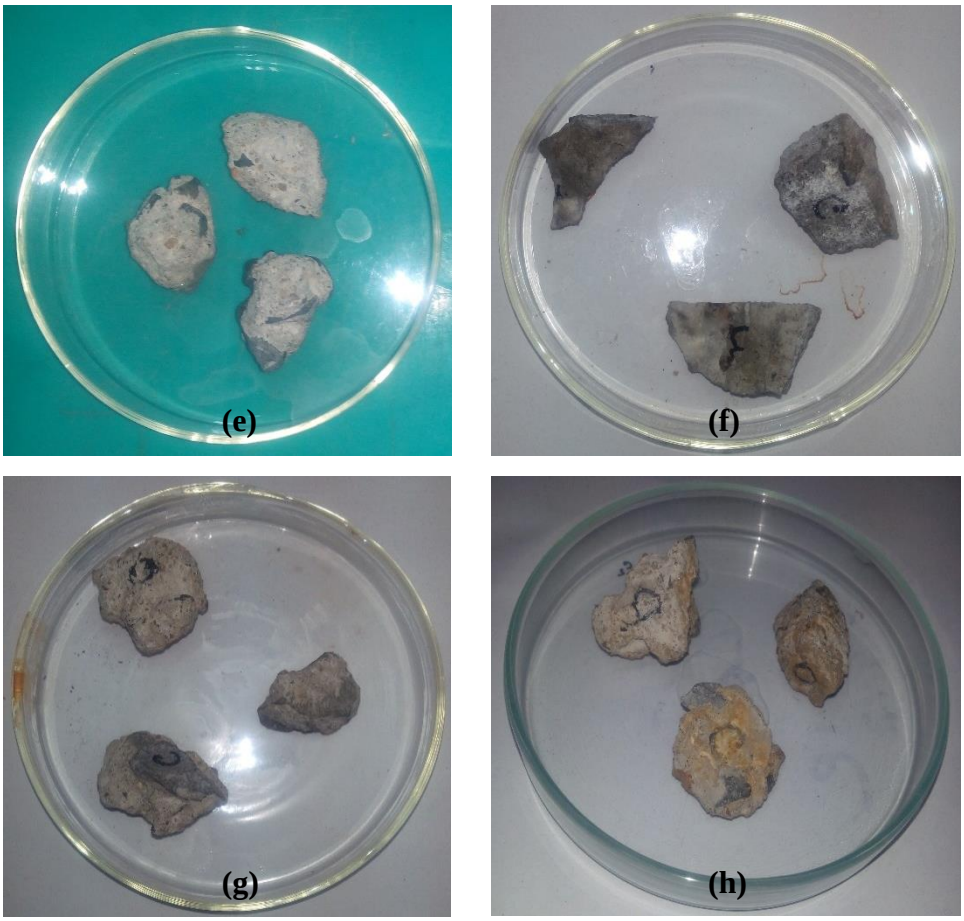

Figure 17: Observed colour changes with their colour codes (as per Geological Rock Colour Chart-Munsell, 2009)

(e) Control- Pinkish gray (5YR 8/1)
(f) Biodeterioration after 1 month- Light greenish gray (5GY 8/1)
(g) Biodeterioration after 2 months- Yellowish gray (5Y 8/1)
(h) Biodeterioration after 3 months- Yellowish gray (5Y 8/1)

It was observed that the concrete pieces of the biodeterioration set-up over the time lost its original colour (as could be seen in control) and became paler and rustier.

5.1.1.2 Weight Loss Percentage (%) :

Control

Time Period	Weight (g)		Weight loss (g)	Weight loss Percentage (%)	Average Weight loss Percentage (%)
	Initial	Final			
After 1 month	6.200	6.190	0.008	0.13	0.67
	8.190	8.185	0.005	0.06	
	5.595	5.493	0.102	1.82	
After 2 months	11.430	11.245	0.185	1.62	1.84
	8.880	8.545	0.335	3.77	
	11.690	11.675	0.015	0.13	
After 3 months	6.880	6.484	0.396	5.76	4.71
	8.940	8.635	0.304	3.40	
	8.940	8.495	0.445	4.97	

Table 1: Weight Loss Percentage of concrete pieces of control over 3 months.

Biodeterioration

Time Period	Weight (g)		Weight loss (g)	Weight loss Percentage (%)	Average Weight loss Percentage (%)
	Initial	Final			
After 1 month	6.190	6.178	0.012	0.19	1.85
	7.590	7.398	0.192	2.53	
	5.770	5.607	0.163	2.83	
After 2 months	8.875	8.534	0.341	3.84	3.13
	12.735	12.232	0.503	3.95	
	12.205	12.008	0.197	1.61	
After 3 months	7.480	6.712	0.768	10.27	9.09
	6.340	5.830	0.510	8.04	
	9.605	8.744	0.861	8.96	

Table 2: Weight Loss Percentage of concrete pieces of biodeterioration over 3 months.

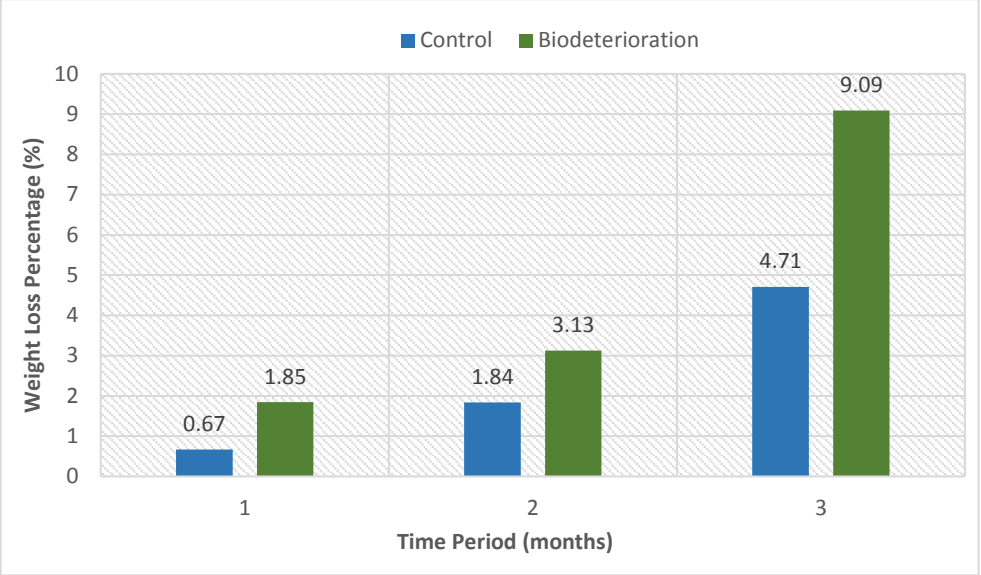

Figure 18: Comparison of Weight Loss Percentage (%) between control and biodeterioration concrete pieces.

From the preliminary study of the concrete cubes over 3 months, it was noted that the weight loss percentage of bio-deteriorated concrete pieces was higher to that of control and the respective concrete pieces were thus getting affected adversely with the fungal growth over time.

5.1.2 Fungal Biodeterioration of Concrete Pieces and its Prevention with Nanocoating (Second 3 months study) :

5.1.2.1 Colour change :

(a) Control

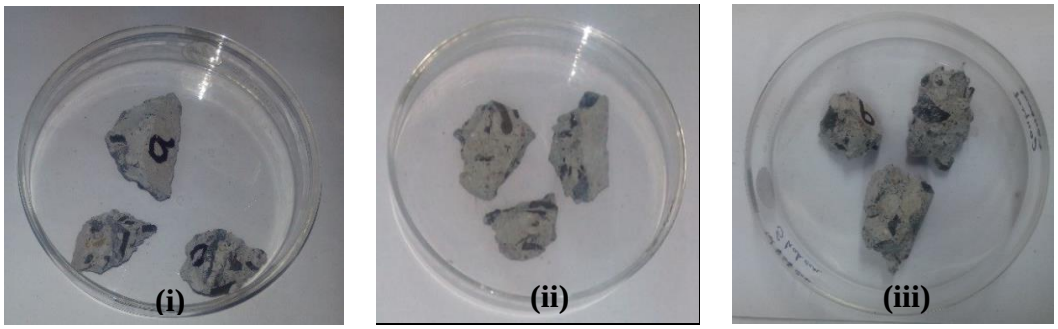

(b) Biodeterioration

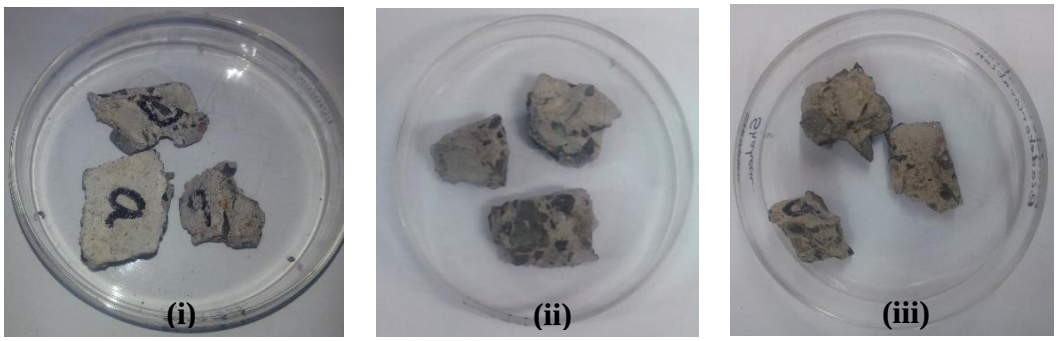

(c) Prevention

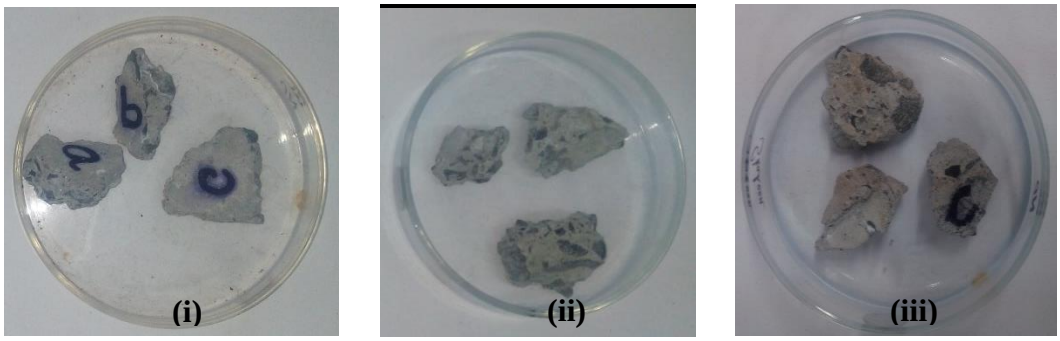

Figure 19: Observed colour changes with their colour codes (as per Geological Rock Colour Chart-Munsell, 2009)

(a) Control : (i) after 1 month- Pinkish gray (5YR 8/1) (ii) after 2 months - Pinkish gray (5YR 8/1) (iii) after 3 months- Pinkish gray (5YR 8/1)

(b) Biodeterioration : (i) after 1 month- Light greenish gray (5GY 8/1) (ii) after 2 months- Light greenish gray (5GY 8/1) (iii) after 3 months- Yellowish gray (5Y 8/1)

(c) Prevention (i) after 1 month- Pinkish gray (5YR 8/1): (ii) after 2 months- Pinkish gray (5YR 8/1) (iii) after 3 months- Yellowish gray (5Y 8/1)

From the colour change observation, it was seen that the control and nanocoated concrete pieces from the prevention set-up retained their colour tone of pinkish gray (5YR 8/1) longer than the biodeteriorated concrete pieces which first turned light greenish gray (5GY 8/1) and then eventually to yellowish gray (5Y 8/1).

5.1.2.2 Weight Loss Percentage (%) :

Control

Time Period	Weight (g)		Weight loss (g)	Weight loss Percentage (%)	Average Weight loss Percentage (%)
	Initial	Final			
After 1 month	6.32 3.44 4.92	6.30 3.43 4.89	0.02 0.01 0.03	0.32 0.29 0.61	0.41
After 2 months	6.35 3.44 4.90	6.33 3.40 4.83	0.02 0.04 0.01	0.32 1.16 0.20	0.56
After 3 months	6.11 3.56 4.87	6.08 3.54 4.83	0.03 0.02 0.04	0.49 0.56 0.82	0.62

Table 3: Weight loss Percentage of concrete pieces of control over 3 months.

Biodeterioration

Time Period	Weight (g)		Weight loss (g)	Weight loss Percentage (%)	Average Weight loss Percentage (%)
	Initial	Final			
After 1 month	7.66 4.35 4.69	7.56 4.23 4.60	0.10 0.12 0.09	1.30 2.76 1.92	1.99
After 2 months	7.66 4.18 4.65	7.42 4.01 4.46	0.24 0.17 0.19	3.13 4.07 4.09	3.76
After 3 months	7.80 4.41 4.70	7.51 4.23 4.53	0.29 0.18 0.18	3.72 4.08 3.83	3.88

Table 4: Weight loss Percentage of concrete pieces of biodeterioration over 3 months.

Prevention

Time Period	Weight (g)		Weight loss (g)	Weight loss Percentage (%)	Average Weight loss Percentage (%)
	Initial	Final			
After 1 month	7.94 4.15 5.15	7.89 4.07 5.08	0.05 0.08 0.07	0.63 1.93 1.36	1.31
After 2 months	7.84 4.15 5.85	7.74 4.08 5.72	0.10 0.07 0.13	1.28 1.69 2.22	1.73
After 3 months	7.93 4.08 5.22	7.87 3.99 5.07	0.06 0.09 0.15	0.76 2.21 2.87	1.95

Table 5: Weight loss Percentage of concrete pieces of prevention over 3 months

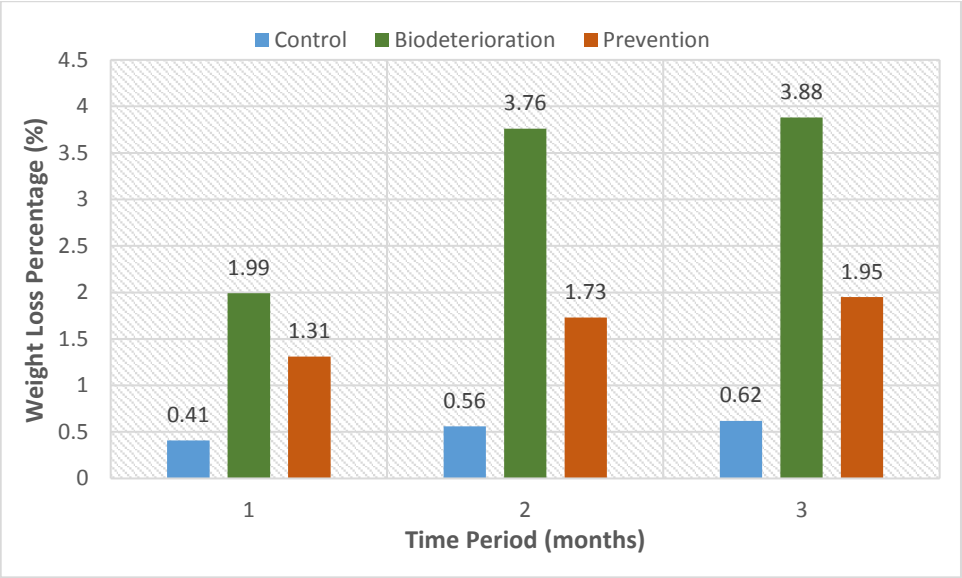

Figure 20: Comparison of Weight Loss Percentage (%) between control, biodeteriorated and nanocoated concrete pieces.

The data and the comparison chart showed that the percentage weight loss (%) of bio-deteriorated concrete pieces, over the 3 months of study, was significantly higher than the nanocoated concrete pieces and the control concrete pieces. The weight loss of concrete pieces of the control set-up was near to negligible.

5.2 Tests and Analysis done on the Concrete cubes :

5.2.1 Humidity measurement :

Time Period	ATMOSPHERIC		HUMIDITY (% RH)			
	Temperature (°C)	Humidity (%RH)	Control	Positive Control	Biodeterioration	Prevention
1st Month	29.4 °C	72.6	74.7	77.2	79.4	80.5
2nd Month	28.2 °C	66.9	69.2	72.8	78.7	77.8
3rd Month	26.0 °C	53.6	69.9	78.8	81.3	79.7
4th Month	22.1 °C	41.2	60.3	68.8	69.9	73.6
5th Month	25.9 °C	48.4	61.1	80.3	82.5	87.7
6th Month	25.6 °C	46.7	54.4	68.6	72.4	70.5

Table 6: Relative Humidity of the atmosphere and inside the set-up boxes of the experiment over the study period of 6 months.

The relative humidity was recorded to be the least in the control set-up, followed by the positive control. The reason being that the concrete cubes in the control set-up were kept dry throughout whereas the cubes in the positive control were moistened periodically with autoclaved distilled water. Humidity was recorded to be the highest in both the biodeterioration and prevention set-up respectively as a considerable volume of media was added initially to these sets for the optimum growth of the inoculated *Aspergillus tamarii*.

5.2.2 pH measurement :

Biodeterioration

Time Period	pH of the media
After 1 month	8
After 2 months	8.5
After 3 months	9
After 4 months	10
After 5 months	12
After 6 months	12

Table 7: Recorded pH of the biodeterioration set-up for 6 months.

Prevention

Time Period	pH of the media
After 1 month	7.5
After 2 months	8
After 3 months	9
After 4 months	10
After 5 months	10
After 6 months	10

Table 8: Recorded pH of the prevention set-up for 6 months.

The initial pH of the media was 7.3± 2 but with the proceeding of the study, the pH of the media of both the biodeterioration and the prevention were noted to have increased making the media more alkaline in nature. An increment in the overall pH for both the cases were thus observed. Luo et al., (2007) studies agreed with this result which shows that when *Trichoderma reesei* interacts with concrete its dissolves $Ca(OH)_2$ (calcium hydroxide) into the growth medium and thus the pH of the media which was 6 initially increased to 13 considerably.

5.2.3 Colour change observation :

The colour change detected in the concrete cubes over time were inferred with the help of the Geological Rock Colour Chart (Munsell, 2009). It was observed that the growth of the fungal species, on the concrete cubes of the biodeterioration and the prevention sets, imparted a significant greenish hue (Light greenish gray) to the cubes which eventually turned to a shade of yellowish gray with longer exposure time.

However the concrete cubes of the control and positive control sets retained their original colour (Pinkish gray) throughout the experiment

Control:

1st Month
Pinkish gray (5YR 8/1)

3rd Month
Pinkish gray (5YR 8/1)

6th Month
Pinkish gray (5YR 8/1)

Positive Control:

1st Month
Pinkish gray (5YR 8/1)

3rd Month
Pinkish gray (5YR 8/1)

6th Month
Pinkish gray (5YR 8/1)

Biodeterioration:

1st Month
Light greenish gray (5GY 8/1)

3rd Month
Yellowish gray (5Y 8/1)

6th Month
Yellowish gray (5Y 8/1)

Prevention:

1st Month
Light greenish gray (5GY 8/1)

3rd Month
Light greenish gray (5GY 8/1)

6th Month
Yellowish gray (5Y 8/1)

Figure 21: Observed colour change of the concrete cube surfaces along with their respective colour codes (as per Geological Rock Colour chart – Munsell, 2009).

5.2.4 Weight loss measurement

Control

Time Period	Weight (g)		Weight loss (g)	Weight loss Percentage (%)	Average Weight loss Percentage (%)
	Initial	Final			
After 1 month	0.876 0.857 0.847	0.868 0.850 0.842	0.008 0.007 0.005	0.913 0.817 0.590	0.773
After 2 months	0.886 0.859 0.862	0.878 0.854 0.853	0.008 0.005 0.009	0.903 0.582 1.044	0.843
After 3 months	0.858 0.829 0.846	0.849 0.818 0.839	0.009 0.011 0.007	1.049 1.327 0.827	1.068
After 4 months	0.820 0.846 0.859	0.811 0.833 0.847	0.009 0.013 0.012	1.098 1.537 1.397	1.344
After 5 months	0.847 0.839 0.863	0.831 0.827 0.851	0.016 0.012 0.012	1.889 1.430 1.391	1.570
After 6 months	0.876 0.869 0.862	0.860 0.855 0.848	0.016 0.014 0.014	1.827 1.611 1.624	1.687

Table 9: Weight loss Percentage (%) of Concrete Cubes for Control set-up.

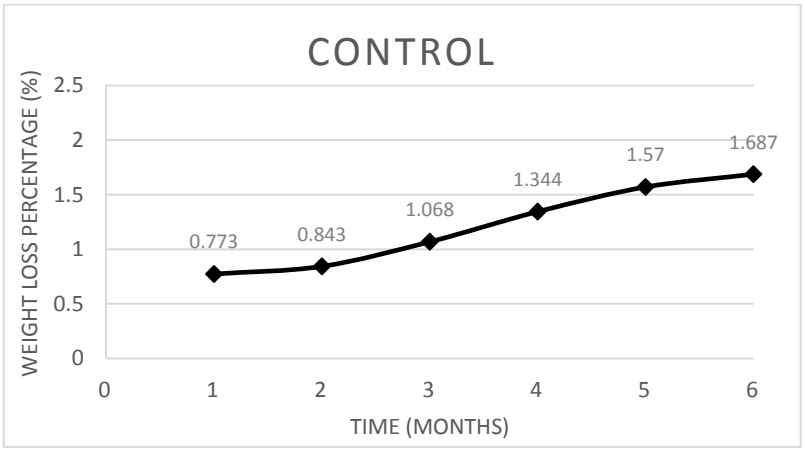

Figure 22: Weight loss Percentage (%) with Time (months) for concrete cubes of Control set-up.

Positive Control

Time Period	Weight (g)		Weight loss (g)	Weight loss Percentage (%)	Average Weight loss Percentage (%)
	Initial	Final			
After 1 month	0.827 0.837 0.827	0.821 0.833 0.824	0.006 0.004 0.003	0.726 0.478 0.363	0.522
After 2 months	0.829 0.830 0.831	0.823 0.824 0.824	0.006 0.006 0.007	0.724 0.723 0.842	0.763
After 3 months	0.834 0.832 0.847	0.824 0.824 0.842	0.010 0.008 0.005	1.199 0.962 0.590	0.917
After 4 months	0.870 0.831 0.858	0.859 0.823 0.852	0.011 0.008 0.006	1.264 0.963 0.699	0.976
After 5 months	0.832 0.841 0.845	0.825 0.833 0.835	0.007 0.008 0.010	0.841 0.951 1.183	0.992
After 6 months	0.849 0.829 0.853	0.837 0.822 0.843	0.012 0.007 0.010	1.413 0.844 1.172	1.143

Table 10: Weight loss Percentage (%) of Concrete Cubes for Positive Control set-up.

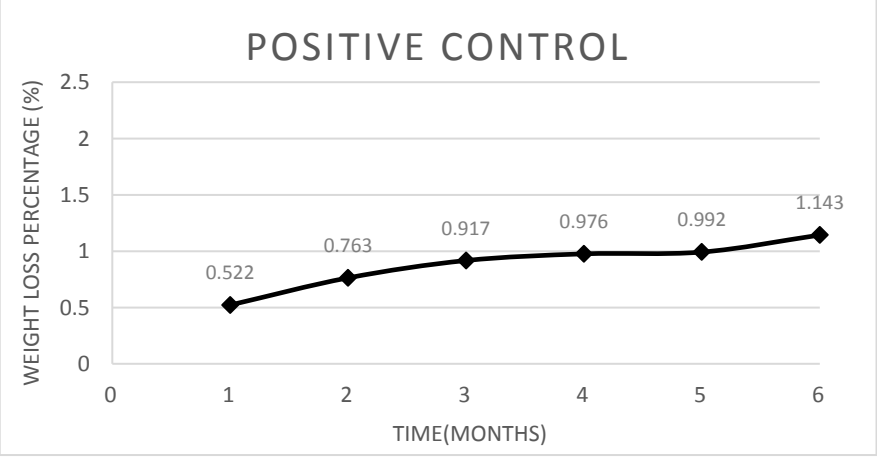

Figure 23: Weight loss Percentage (%) with Time (months) for concrete cubes of Positive Control set-up.

Biodeterioration

Time Period	Weight (g)		Weight loss (g)	Weight loss Percentage (%)	Average Weight loss Percentage (%)
	Initial	Final			
After 1 month	0.833 0.870 0.853	0.828 0.861 0.847	0.005 0.009 0.006	0.600 1.035 0.703	0.779
After 2 months	0.847 0.853 0.844	0.835 0.842 0.831	0.012 0.011 0.013	1.416 1.290 1.540	1.415
After 3 months	0.876 0.862 0.855	0.861 0.851 0.842	0.015 0.011 0.013	1.712 1.276 1.520	1.503
After 4 months	0.838 0.859 0.842	0.824 0.847 0.827	0.014 0.012 0.015	1.671 1.397 1.782	1.617
After 5 months	0.855 0.846 0.829	0.841 0.829 0.816	0.014 0.017 0.013	1.637 2.010 1.568	1.738
After 6 months	0.842 0.879 0.869	0.826 0.858 0.852	0.016 0.021 0.017	1.900 2.389 1.956	2.082

Table 11: Weight loss Percentage (%) of Fungal Infected Concrete Cubes for Biodeterioration set-up.

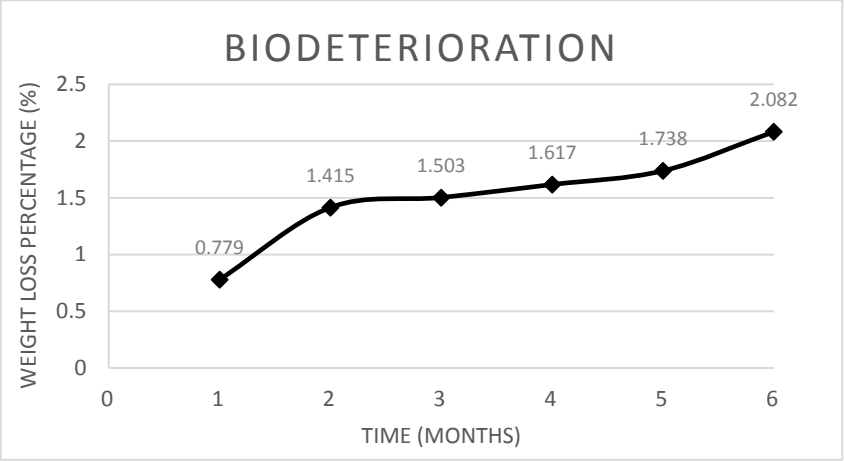

Figure 24: Weight loss Percentage (%) with Time (months) for biodeteriorated concrete cubes.

Prevention

Time Period	Weight (g)		Weight loss (g)	Weight loss Percentage (%)	Average Weight loss Percentage (%)
	Initial	Final			
After 1 month	0.846 0.831 0.840	0.839 0.824 0.834	0.007 0.007 0.006	0.827 0.842 0.714	0.794
After 2 months	0.818 0.856 0.868	0.803 0.843 0.857	0.015 0.013 0.011	1.834 1.519 1.267	1.540
After 3 months	0.859 0.868 0.832	0.846 0.853 0.816	0.010 0.015 0.016	1.164 1.728 1.923	1.605
After 4 months	0.848 0.847 0.886	0.837 0.830 0.871	0.011 0.017 0.015	1.297 2.007 1.693	1.666
After 5 months	0.859 0.869 0.846	0.843 0.854 0.830	0.016 0.015 0.016	1.863 1.726 1.891	1.827
After 6 months	0.835 0.860 0.839	0.814 0.843 0.820	0.018 0.017 0.019	2.156 1.977 2.265	2.133

Table 12: Weight loss Percentage (%) of Nanocoated Concrete Cubes for Prevention set-up.

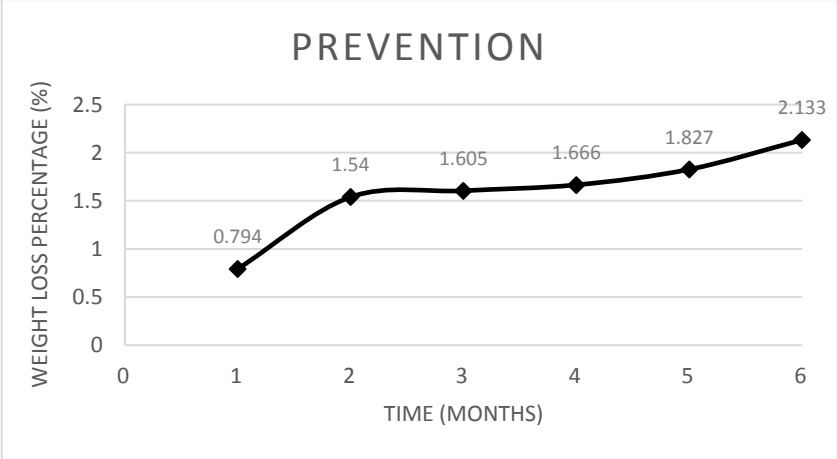

Figure 25: Weight loss Percentage (%) with Time (months) for nanocoated concrete cubes.

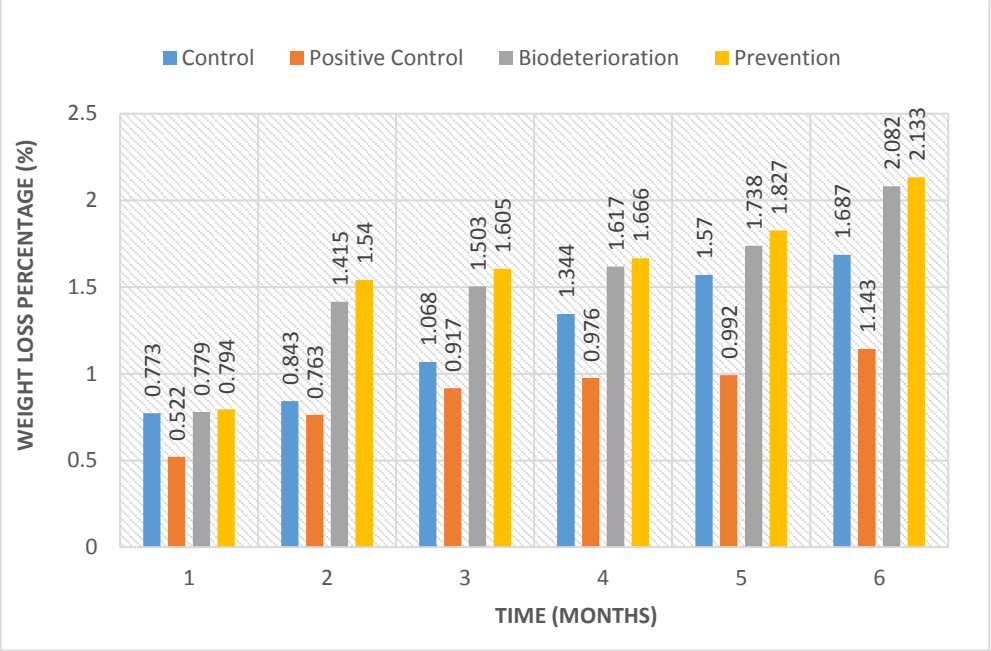

Figure 26: Comparison of percentage weight loss (%) with time (months) of concrete cubes from the respective experimental set-ups.

From the data tables and the data curves, it was inferred that over the period of 6 months the concrete cubes of each experimental set has undergone weight loss with variation in each of the set-ups. The weight loss in nanocoated concrete cubes were observed to be the highest, followed by biodeteriorated cubes, control and positive control cubes.

The weight loss percentage result agreed with some similar studies conducted by Gu et al., (1998), and Harbulakova et al., (2013) which concluded that biodeterioration of concrete resulted in their weight loss. The study done by Harbulakova et al., (2013) also concluded that the concrete when kept in distilled water showed almost negligible changes in weight over time.

Moreover the loss of weight in concrete cubes of control can be explained with the study conducted by Gesoglu et al.,(2015), stating that drying shrinkage, which is the loss of absorbed water in concrete with time, affects its weight adversely. It was also deduced that this volumetric change in concrete depended on the drying duration, water to cement ratio, cement composition, aggregate properties, admixtures, curing temperature, degree of hydration and relative humidity.

5.2.5 Stereo Microscope :

Figure 27: Stereo microscopic image of concrete cube surface from the control set-up.

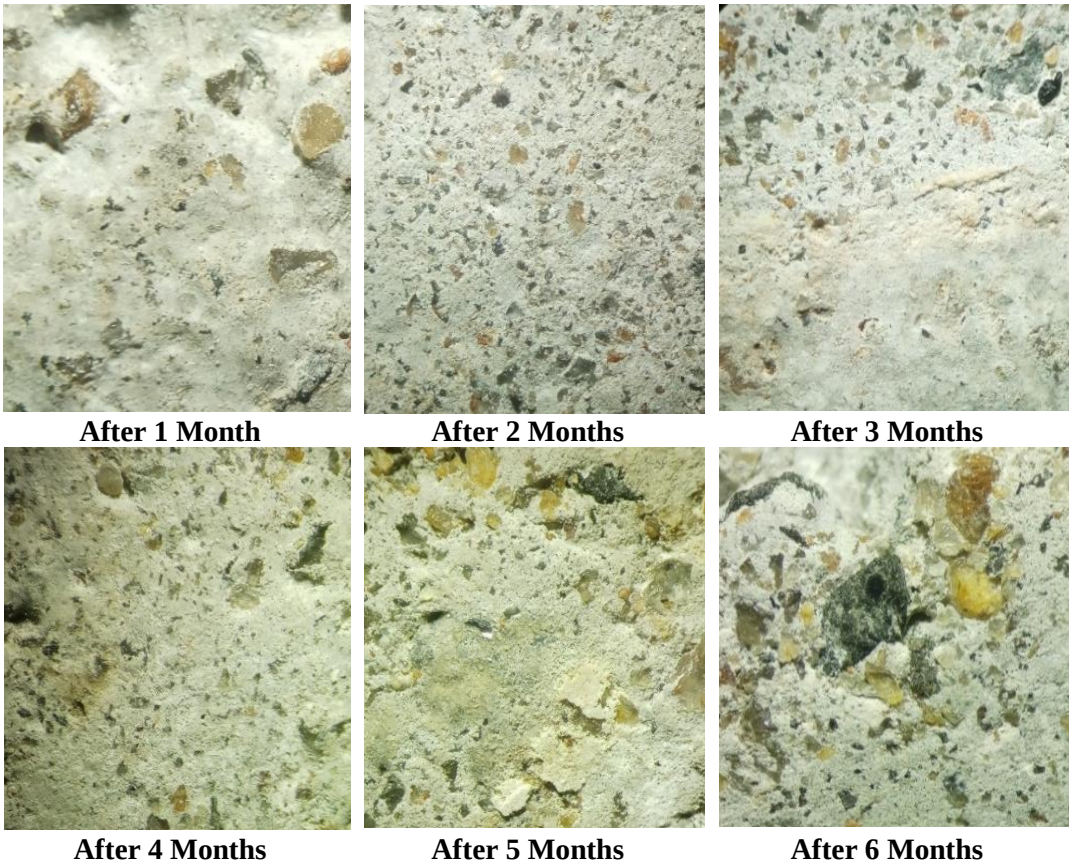

Figure 28: Stereo microscopic images of concrete cube surfaces infected by fungus from the biodeterioration set-up.

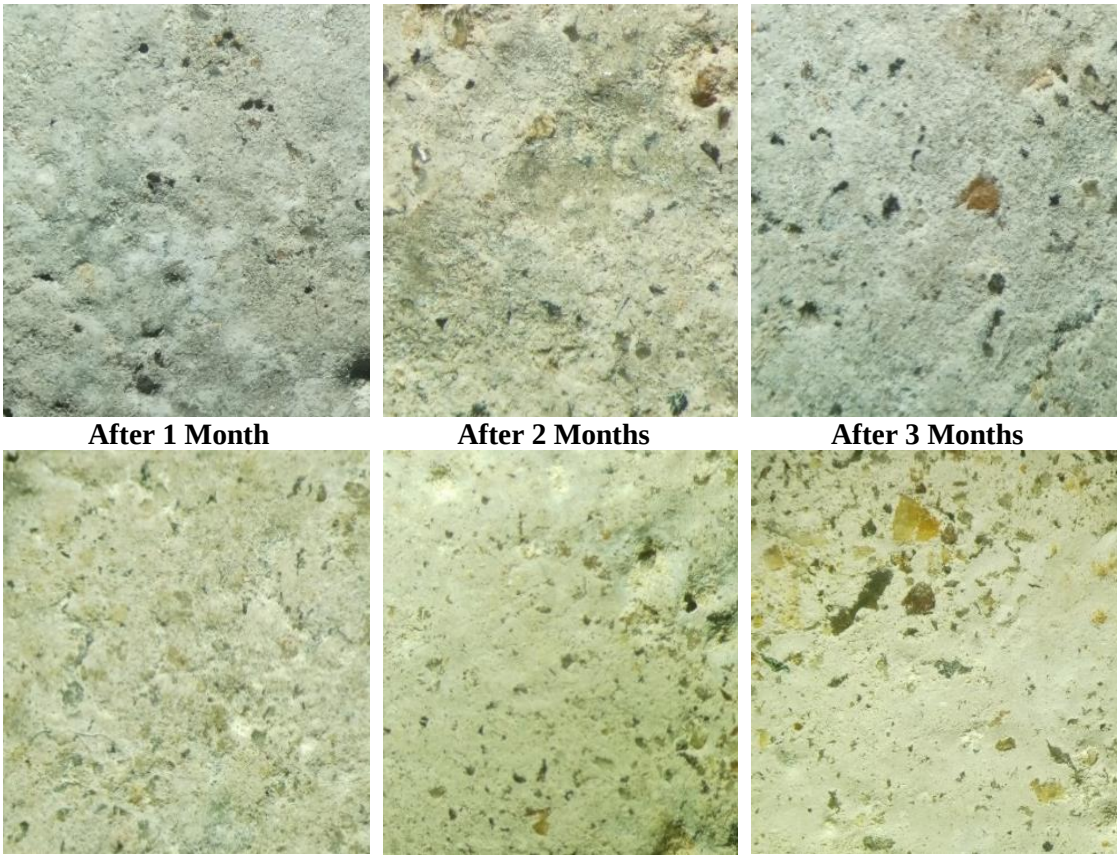

Figure 29: Stereo microscopic images of nanocoated concrete cube surfaces infected by fungus from the prevention set-up.

As compared to control, the concrete surface of the biodeterioration as well as of prevention were seen to have got exposed and rough. The growth of micro-organisms on concrete exposes the concrete surface thus increasing the porosity and reducing the protective layer that covers the concrete surface, making it vulnerable to cracking and other mechanical damages (Sanchez et al.,2008).

The intensity of roughness was observed more in biodeteriorated concrete cubes rather than in the nanocoated ones under the stereo microscope. The surface of the cubes of biodeterioration developed cavities as can be seen in the images (Figure 28). Concrete is more susceptible to microbiological attack with a high rate of fungal growth mainly because of its initial porosity and chemical composition. In the case of nanocoated concrete cubes, the coating provided a surface protective layer (Aldosari et al., 2018) which inhibited the growth of the fungus to a considerable limit thus revealing much less of the concrete cube surface.

5.2.6 Compressive strength test :

Initial : (After drying for 3 days)

Peak Load (kN)	**Compressive Strength (N/mm^2)**	**Average Compressive Strength (N/mm^2)**
155.4	31.71	30.21
145.4	29.67	
143.3	29.25	

Table 13: Initial Compressive strength of concrete cubes.

Control

Time Period	Peak Load (kN)	Compressive Strength (N/mm^2)	Average Compressive Strength (N/mm^2)
After 1 month	157.5 146.2 152.7	32.14 29.84 31.16	31.05
After 2 months	149.2 149.5 164.1	30.45 30.51 33.49	31.48
After 3 months	148.8 159.5 167.4	30.37 32.56 34.16	32.36
After 4 months	163.5 157.4 164.2	33.37 32.12 33.51	33.00
After 5 months	170.4 155.3 166.6	34.78 31.69 34.00	33.49
After 6 months	160.0 164.1 172.8	32.65 33.49 35.26	33.80

Table 14: Peak load and Compressive Strength of concrete cubes from Control set-up.

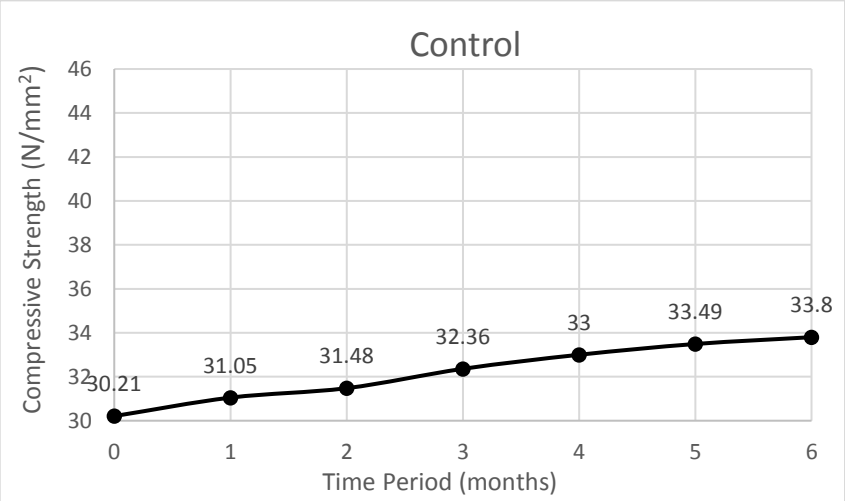

Figure 30: Compressive strength of control concrete cubes with respect to time.

Positive Control

Time Period	Peak Load (kN)	Compressive Strength (N/mm^2)	Average Compressive Strength (N/mm^2)
After 1 month	159.4 167.1 149.7	32.53 34.10 30.55	32.39
After 2 months	174.8 159.0 149.5	35.67 32.45 30.51	32.87
After 3 months	151.9 174.5 177.5	31.00 35.61 36.22	34.28
After 4 months	179.9 174.6 185.2	36.71 35.63 37.80	36.71
After 5 months	202.5 196.6 223.2	41.33 40.12 45.55	42.33
After 6 months	209.3 233.8 221.7	42.71 47.71 45.25	45.22

Table 15: Peak load and Compressive Strength of concrete cubes from Positive Control set-up.

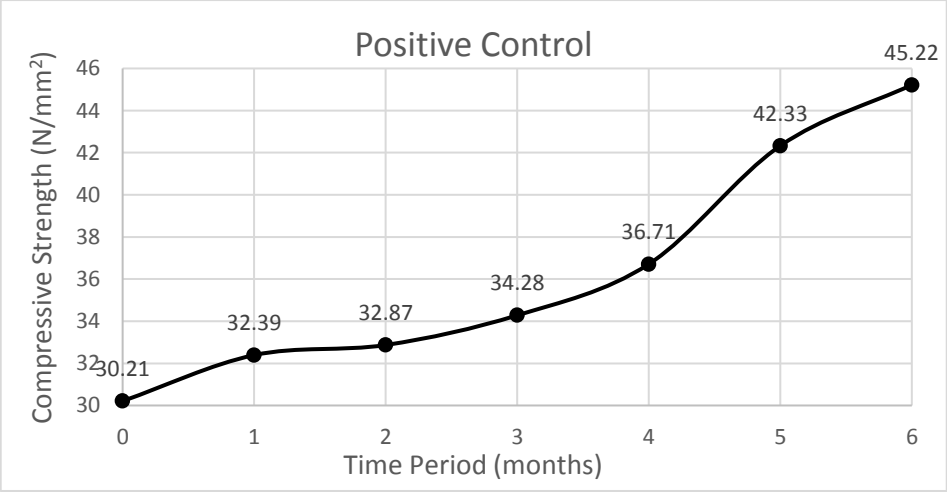

Figure 31: Compressive strength of positive control concrete cubes with respect to time.

Biodeterioration

Time Period	Peak Load (kN)	Compressive Strength (N/mm^2)	Average Compressive Strength (N/mm^2)
After 1 month	160.6 149.5 134.3	32.78 30.51 27.41	30.23
After 2 months	122.9 179.5 161.8	25.08 36.63 33.02	31.58
After 3 months	142.6 184.4 182.9	29.10 37.63 37.33	34.69
After 4 months	210.1 151.3 152.3	42.88 30.88 31.08	34.95
After 5 months	152.7 179.0 185.5	31.16 36.53 37.86	35.18
After 6 months	190.8 187.1 176.0	38.94 38.18 35.92	37.68

Table 16: Peak load and Compressive Strength of concrete cubes from Biodeterioration set-up.

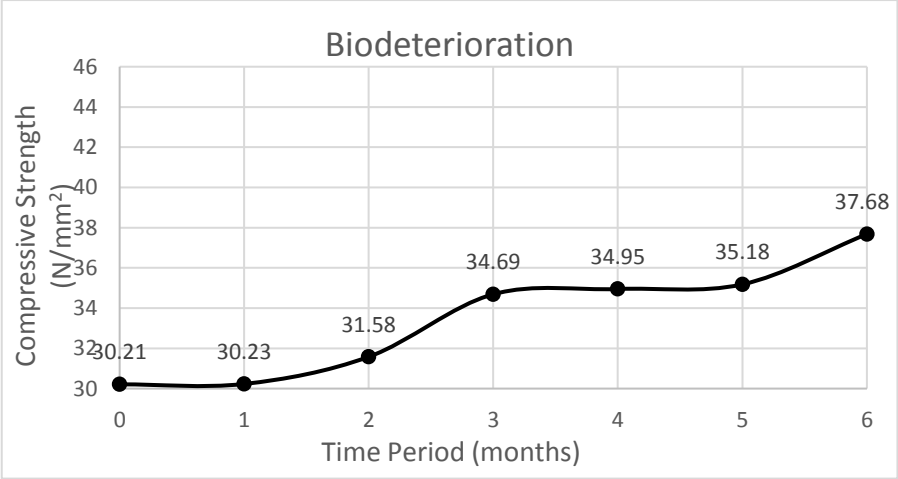

Figure 32: Compressive strength of biodeteriorated concrete cubes with respect to time.

Prevention

Time Period	Peak Load (kN)	Compressive Strength (N/mm^2)	Average Compressive Strength (N/mm^2)
After 1 month	143.1 156.5 144.6	29.20 31.94 29.51	30.22
After 2 months	173.6 148.9 150.0	35.43 30.39 30.61	32.14
After 3 months	160.5 183.9 156.6	32.76 37.53 31.96	34.08
After 4 months	192.7 179.0 191.2	39.33 36.53 39.02	38.29
After 5 months	194.4 198.5 190.2	39.67 40.51 38.82	39.67
After 6 months	206.0 188.3 205.4	42.04 38.43 41.92	40.80

Table 17: Peak load and Compressive Strength of concrete cubes from Prevention set-up.

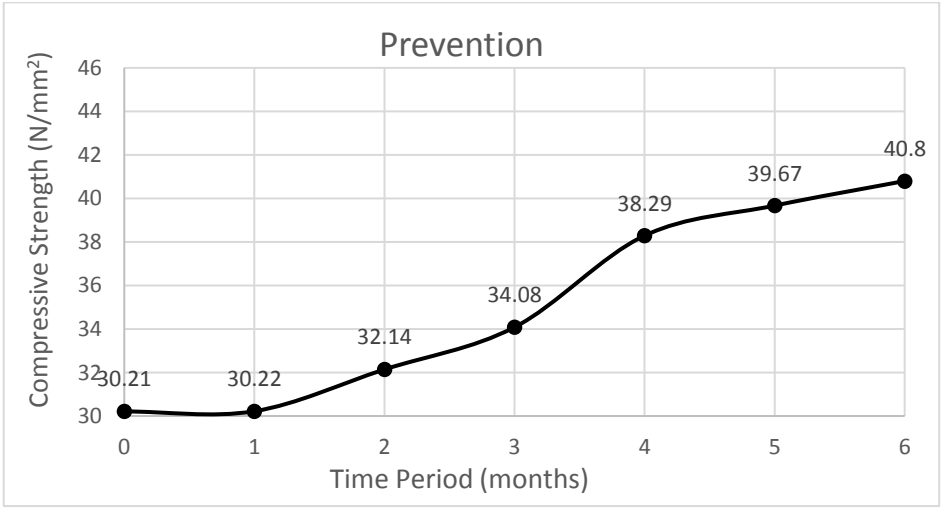

Figure 33: Compressive strength of nanocoated concrete cubes with respect to time.

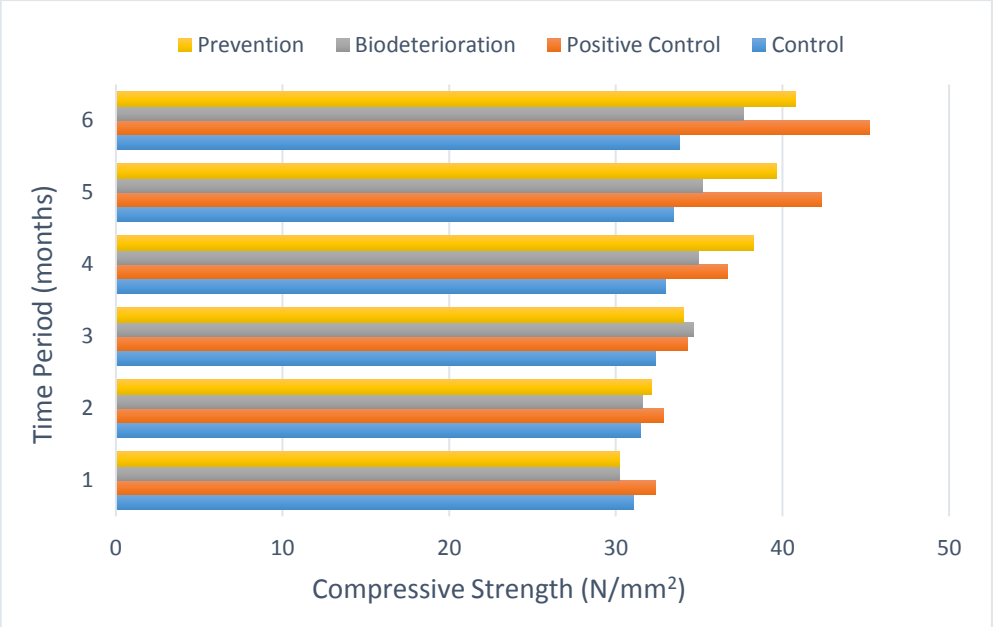

Figure 34: Comparison of compressive strength with time, of concrete cubes from the respective experimental set-ups.

An increase in the compressive strength from the initial compressive strength of 30.21 N/mm^2 was observed in all the concrete specimens. For control the change in compressive strength is not much prominent as compared to the other specimens. For the positive control, where distilled water was added periodically and fungal activity was absent, the compressive strength increase was observed to be the highest followed by nanocoated concrete cubes. The compressive strength increase of biodeteriorated cubes were the least of all the specimens.

This gradual increment in compressive strength in biodeterioration, prevention and positive control set-up could be justified by the reason that all the cubes of these set-ups were kept in an environment where the facilitation of continuous hydration was possible. Hydration is the process consisting of chemical reaction series that occurs between the cement and water, where the water molecules and the major components of cement forms chemical bonds to harden the concrete. In the study, distilled water added to the positive control and the cubes kept in aqueous media in biodeterioration and prevention sets stimulated the process of hydration thus resulting in the rise of compressive strength over the time period of 6 months. In a study conducted by Harbulakova et al.,(2013) , a similar kind of result was observed, where the concrete cubes were immersed in wastewater and

their compressive strength increased with time. Moreover they found that the biocorrosion activity on their high grade concrete cubes was more prominent after a longer exposure (18 months) of the cubes to the wastewater which resulted in an enormous drop in the compressive strength.

Also from the data, the compressive strength increase of nanocoated cubes was noted to be higher than that of the biodeteriorated cubes. Application of organic polymer layer on concrete may not prevent the growth of fungus completely as it can not only get degraded easily but also can provide a susceptible environment for the fungus to grow (Aldorasi el al., 2018). The incorporation of inorganic nanoparticle in a polymer improves the barrier property which slows down the degradation of the polymer (Pan et al., 2017) thus slowing down the fungal growth. This infers that the nanocoating provided an inhibition layer for the fungus to affect the cube much less adversely as compared to the biodeteriorated one which in turn affects its compressive strength.

5.2.7 Scanning Electron Microscope (SEM) :

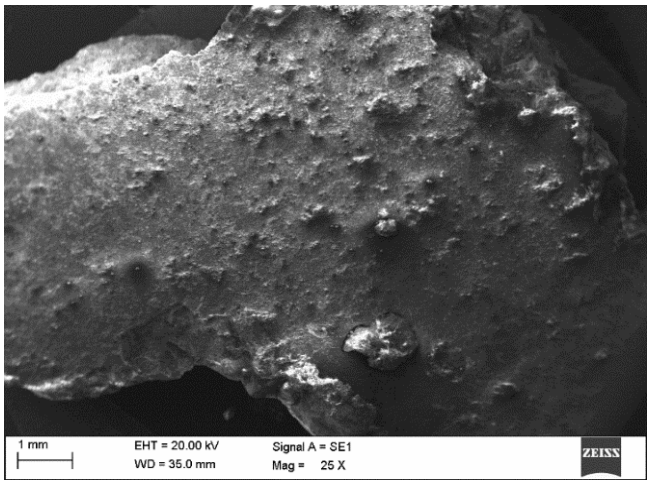

Figure 35: SEM image of concrete from the control set-up

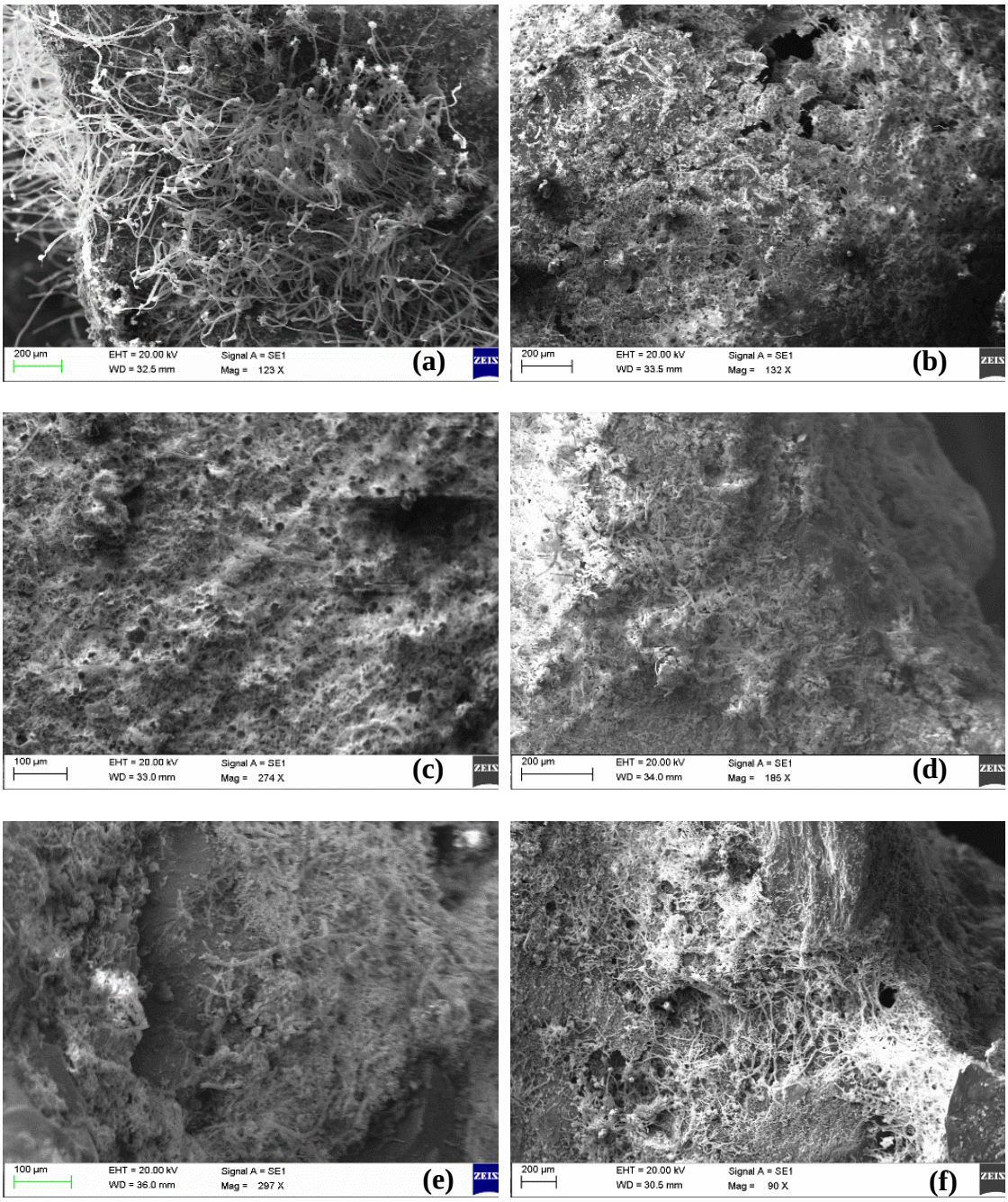

Figure 36: SEM images of concrete from the biodeterioration set-up (a) after 1 month (b) after 2 months (c) after 3 months (d) after 4 months (e) after 5 months (f) after 6 months.

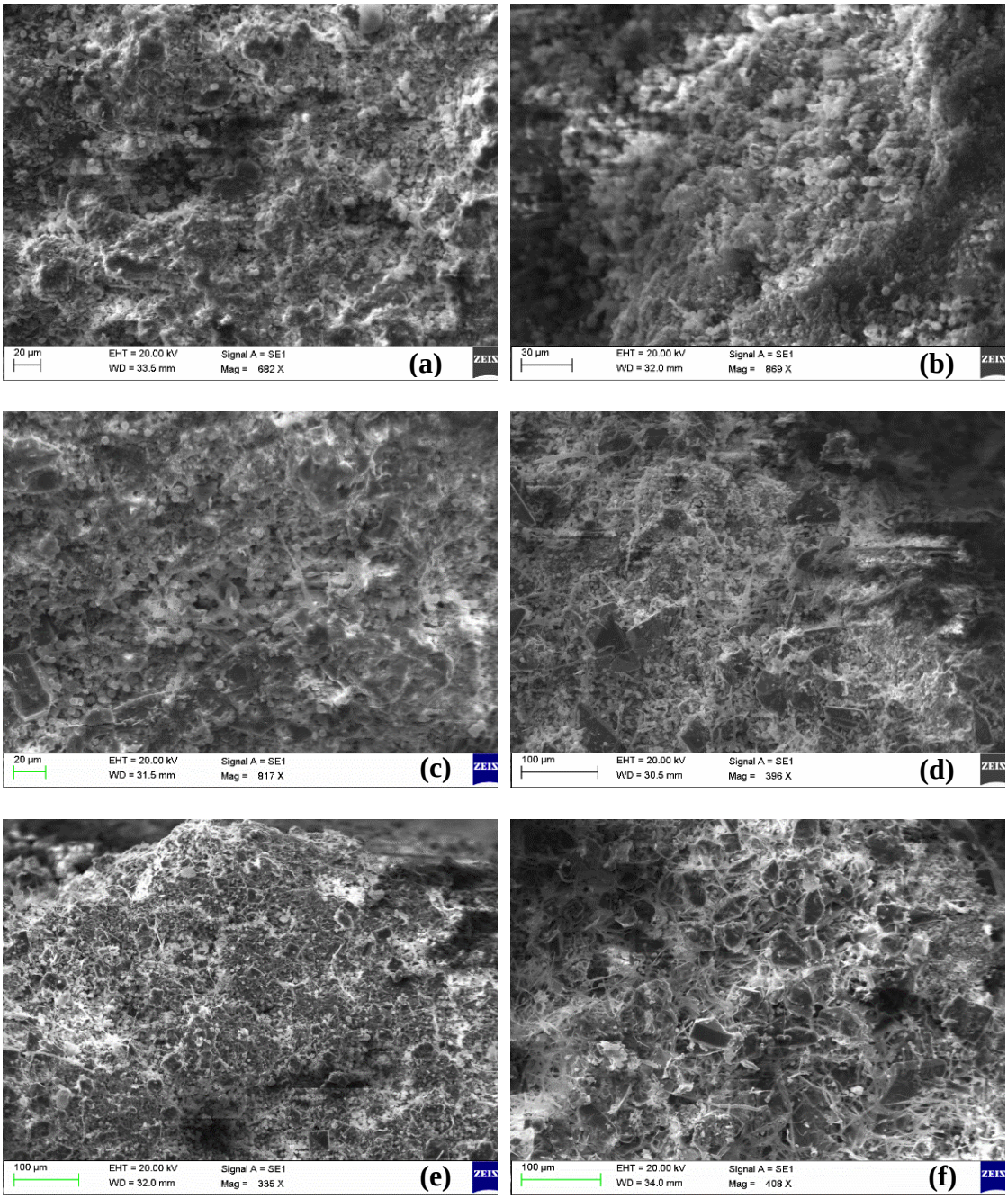

Figure 37: SEM images of concrete from the prevention set-up (a) after 1 month (b) after 2 months (c) after 3 months (d) after 4 months (e) after 5 months (f) after 6 months

The examination of concrete pieces under Scanning Electron Microscope showed that the the hyphae and spore developed with time. The images showed the colonization of *Aspergillus tamarii* on the concrete surface spreading extensively at the end of each month.

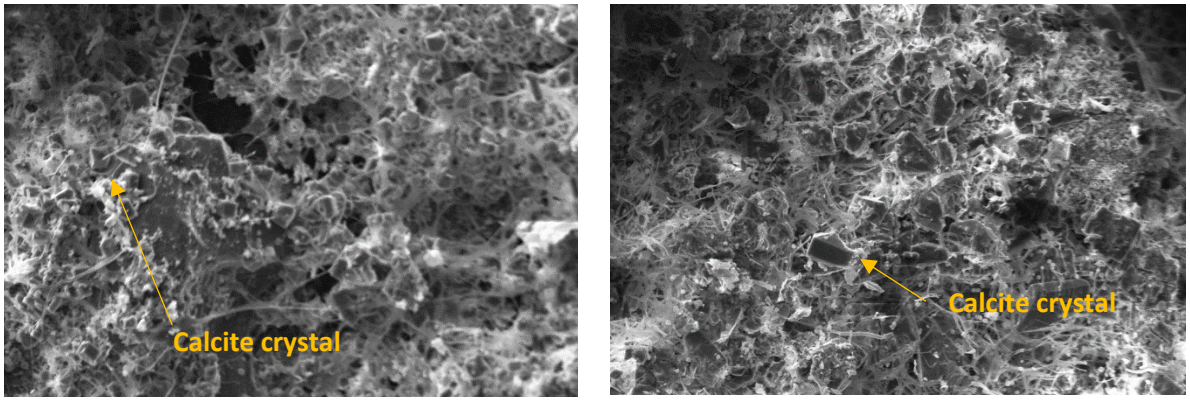

Figure : Calcite crystal formation seen in the SEM images of (a) biodeteriorated concrete cubes and (b) nanocoated concrete cubes infected by *Aspergillus tamarii*.

In synthetic, environmental and biological systems calcite crystallization is a fundamental phenomenon where carbonation is the prime reason for this in the cement system (Jiang et al, 2015). The abundant calcium ions, their source being the hydration products, calcium silicate hydrate and portlandite, reacts with the carbon dioxide of the air, producing calcium carbonate crystals.

Moreover a study conducted by Virrecchia, (2000), showed that saprophytic organisms, mainly fungi requires calcium ions for the growth of their hypha. Thus fungus growing on metamorphic rocks and limestones excreted organic acids which degraded these rocks to precipitate calcium minerals. These calcium minerals were primarily calcium carbonate and calcium oxalate which accumulated on the surface of the rocks as crystals thus inferring that calcite crystal formation is also contributed by fungal activity.

5.2.8 Fourier Transform Infrared Spectroscopy (FTIR) :

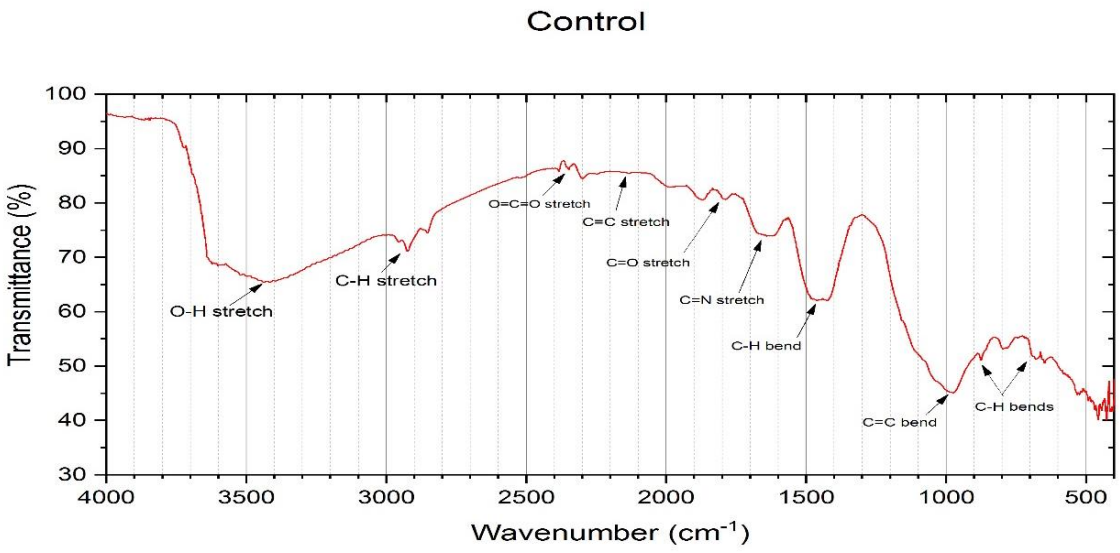

Figure 38: IR transmittance spectrum of concrete for control set-up.

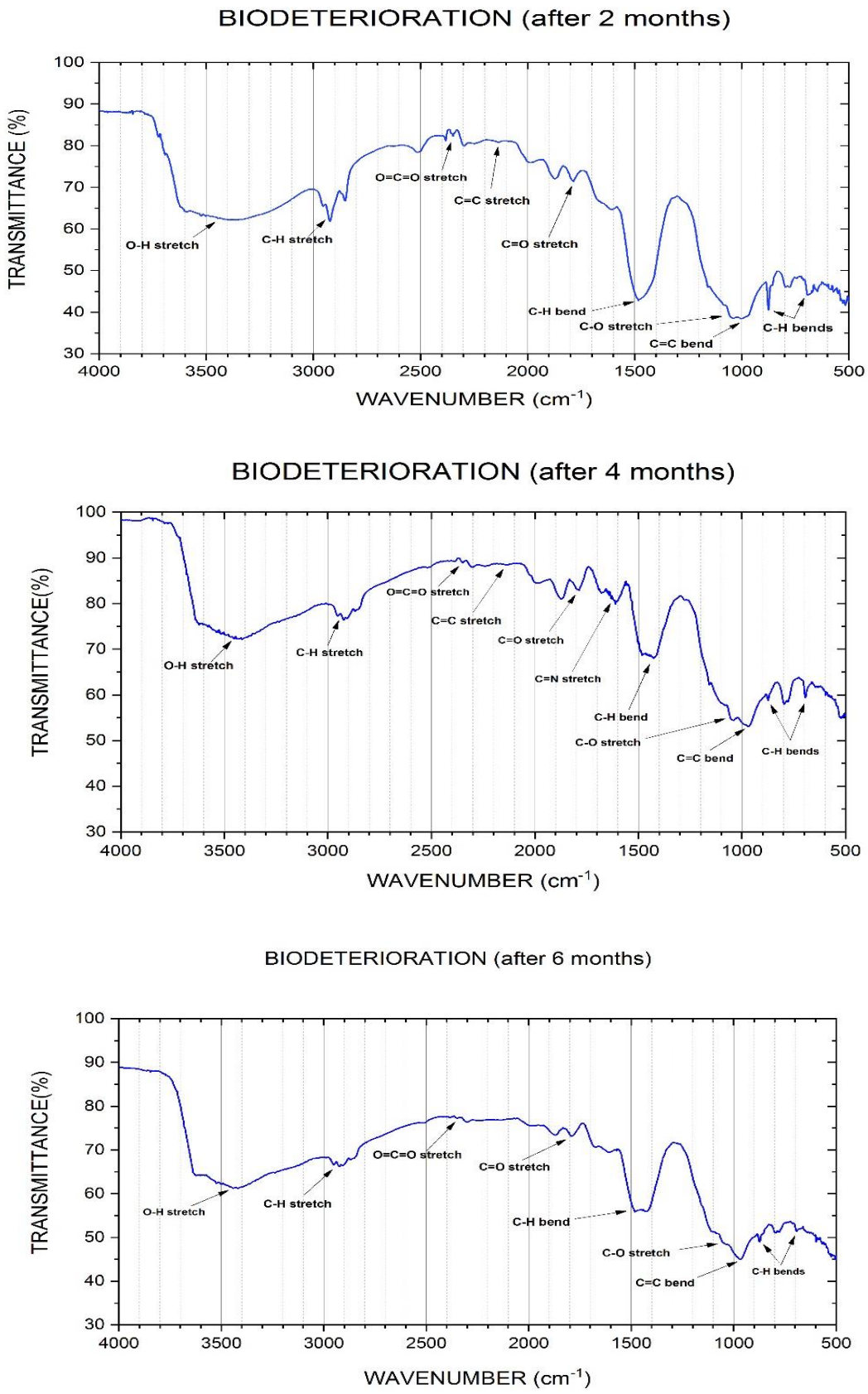

Figure 39: IR transmittance spectrums of concrete for biodeterioration set-up.

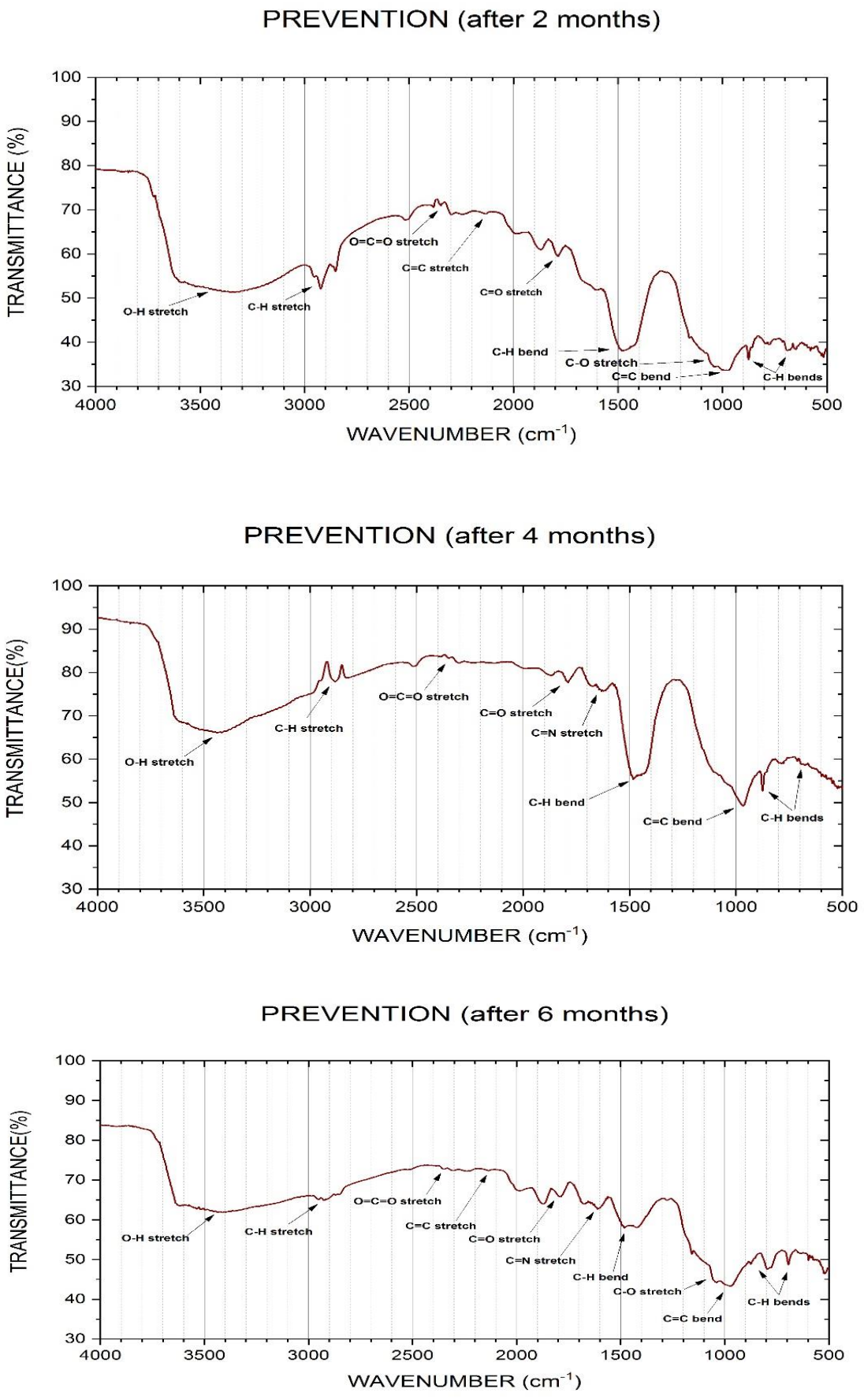

Figure 40: IR transmittance spectrums of concrete for prevention set-up.

From the graphs, a mid IR regional (500-4000 cm^{-1}) spectrum can be visualized. This is ideal for the interpretation of the fundamental structures of specimens and the localization of prominent delineated absorption bands of organic functional groups. According to the IR Correlational chart (Derrick et al.,1955), The spectrum is mainly divided into two regions based on the wavenumber (cm^{-1}). The bands detected in the range of 4000 cm^{-1} to 1300 cm^{-1} falls in the group frequency region whereas the bands detected in the range of 1300 cm^{-1} to 500 cm^{-1} falls in the fingerprint region. Hydrogen stretching vibrations consisting of only two atoms shows their principal absorptions bands from 4000 cm^{-1} to 2500 cm^{-1}. The intermediate frequency range of 2500 cm^{-1} to 1500 cm^{-1} shows the unsaturated region which primarily consists of triple bond frequencies (2500 cm^{-1} to 2000 cm^{-1}) and double bond frequencies (2000 cm^{-1} to 1540 cm^{-1}). Many functional group bands can also be detected in the 1350 cm^{-1} to 650 cm^{-1} frequency.

Broad envelope type bands centered around 3400 cm^{-1} represents hydroxyl groups. The presence of very broad bands in this regions in all the spectral graphs of the tested specimens infers the presence of carboxylic acids. The bands in the biodeterioration were less broad as compared to those of the ones in prevention spectral graphs.

The region of 3200 cm^{-1} to 2800 cm^{-1} is known as the C-H stretching region. The prominent stretching (3000 cm^{-1} to 2890 cm^{-1}) seen in all the spectral graphs of the specimens infers the presence of saturated carbon groups such as methyl and methylene (both symmetric and asymmetric) groups. The sharp C-H stretches in control IR spectrum near 2925 cm^{-1} and 2850 cm^{-1} indicates the presence of both symmetric and asymmetric methylene groups. Similar sharp peaks are can be noticed in the IR spectrums of the biodeteriorated and nanocoated cubes from the biodeterioration and prevention set-ups respectively, which can be seen to get broaden after 4 months and 6 months.

In the window region extending from 2800 cm^{-1} to 1800 cm^{-1}, atmospheric carbon dioxide or O=C=O stretch at 2340 cm^{-1} can be seen in all the specimens. Here also the sharp doublets can be seen to gradually flatten after 4 months and 6 months in biodeterioration and prevention.

The carbon double bond region (1800 cm^{-1} to 1500 cm^{-1}) showing the presence of C=O and the C=N stretchings in all the specimens as well as in control.

The nature of the IR spectrums of control and the specimens showed significant chemical changes that occurred after the fixed intervals of time.

5.2.9 Energy Dispersive X-Ray Fluorescence Spectroscopy (EDXRF) :

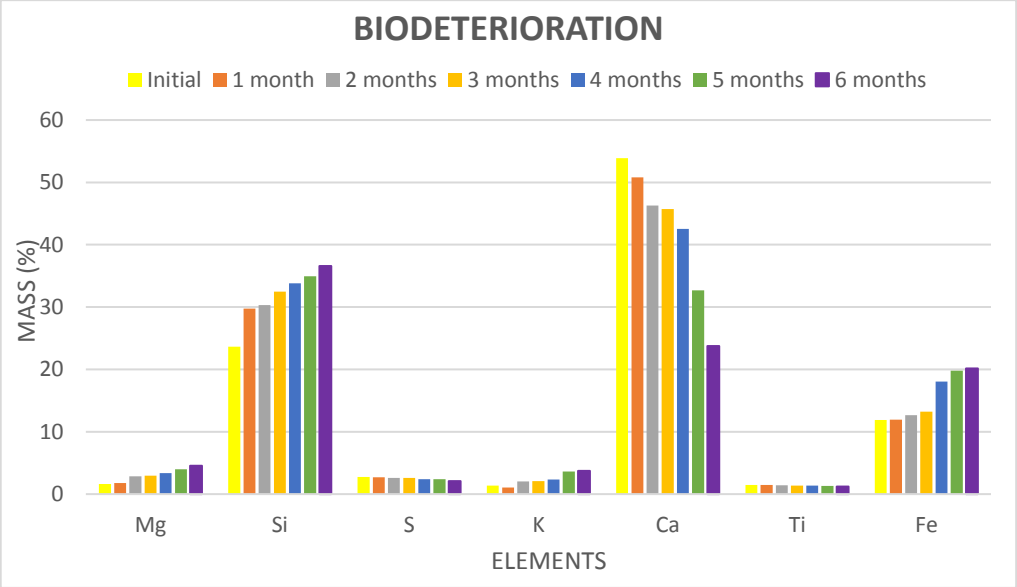

Figure 41: Mass percentage of different elemental contents of biodeteriorated concrete cubes.

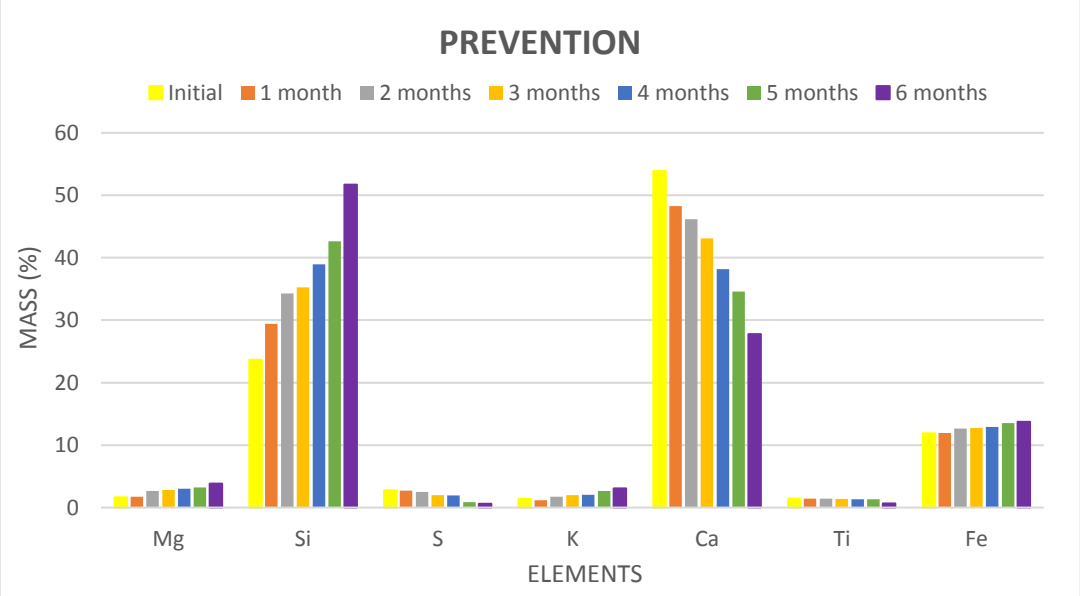

Figure 42: Mass percentage of different elemental contents of nanocoated concrete cubes.

According to the EDXRF results the major elements whose composition variability was prominently detected were silicon, calcium, magnesium, iron, sulphur and potassium.

The composition of titanium in all the specimens were detected but its compositional change was minimal as compared to the rest. Apart from these, trace amounts of copper, manganese, zinc, chromium and nickel were noted initially but these eventually disappeared with time.

The main sources of the detected major elements in concrete are : silicon from Portland cement and sand (SiO_2), calcium, magnesium and iron from Portland cement, and sulphur from gypsum used in Portland cement.

The decrease in mass fraction (%) of calcium was due to the fungal activity of *Aspergillus tamarii* on both the sets of biodeteriorated and nanocoated cubes. In a study conducted by Adeyemi et al., (2005), fungal growth of three different species which included *Aspergillus niger* on mineral rocks of apatite, galena and obsidian showed that organic acids (oxalic and malic acid) produced by the hyphae of these fungi helped in the dissolution of calcium along with the precipitation of crystals of calcium oxalates. However, the rate of decrease of calcium in nanocoated concrete cubes as compared to that of biodeteriorated ones shows that the silicon dioxide nanocoating to some extent provided a barrier for the complete dissolution action of these organic acids upon concrete.

Though biological processes and alike stimulates the weathering of silica and silicates from rocks (Brehm et al., 2005), silicon compounds such as aluminosilicates, may inhibit the metabolism of microbes (Marshman & Marshall, 1981). Fomina et al., (2007c) obtained that species of *Alternaria, Cladosporium and Aspergillus* colonizing the concrete utilized for radioactive waste barrier in Chernobyl facilitated the leaching of calcium, silicon, aluminium and iron and in their microenvironment reprecipitated silicon and calcium.

Grayston and Wainwright (1987) obtained that *Aspergillus niger* and *Trichoderma harzanium* in mixed culture with *Mucor flavus* and various other soil fungi, had the ability to oxidize elemental sulphur into thiosulphate and sulphate in vitro. This may account for the slight fall in mass fraction of sulphur.

Another study conducted by Fomina et al.,(2004) suggested that the fungus *Beauveria caledonica* through a ligand-promoted mechanism of overexcreted organic acids, solubilized copper, cadmium, zinc and lead into their corresponding oxides. This explains the gradual amount decrement of zinc and copper in the study.

CHAPTER VI

CONCLUSION

The assessment of growth of the fungal species, *Aspergillus tamarii* and its effects on concrete followed by its effective prevention using silicon oxide nanoparticles was thoroughly and successfully investigated for a period of 6 months.

The results of the investigation concluded that:

pH :- media of biodeterioration showed more alkalinity than the prevention set-up due to more leaching and dissolution of $Ca(OH)_2$ due to fungal activity. Hence it was inferred that the fungal deterioration was higher in the biodeteriorated concrete cubes than the nanocoated concrete cubes..

Colour Change Observation :- the colour changes in the biodeteriorated concrete cubes were more visually prominent than those of the prevention ones.

Weight Loss Percentage :- the weight loss in prevention was 1.8% whereas in biodeterioration, it was 1.5 % followed by 1.2% in control and 0.9 % in positive control.

Stereo microscope and Scanning Electron Microscope :- the images obtained from the stereo microscope showed clear exposure and roughening of the surface in biodeterioration cubes more than those of the nanocoated cubes. SEM images showed the dense colonization of *Aspergillus tamarii* on the concrete surfaces.

Compressive strength test :- the compressive strength of the nanocoated cubes was 1.8 % higher than those of the biodeteriorated cubes.

FTIR and EDXRF :- both the analysis showed the redistribution of elements and chemical bonds in the concrete cubes with time. In EDXRF it was seen that the amount of calcium leaching out in biodeterioration was higher than that of the nanocoated cubes.

Thus from the experimental evidences and results the nanocoating which was applied on the concrete cubes having the binder, nanoparticles and water ratio of 1:0.5:2, was found to be effective against the biodeterioration of the concrete cubes as proposed in the objective of this study initially.

CHAPTER VII

FUTURE SCOPE OF STUDY

This investigation of fungal biodeterioration on concrete and its prevention using nanoparticles can be a helpful source of various further studies in the near future. There is a scope for the following activities that could be carried out regarding this field of topic namely:

- Biodeterioration study of concrete by other microbial communities can be examined.
- Other prospects and techniques regarding prevention of fungal biodeterioration of concrete can be studied.
- If the time period of the investigation can be further extended, then better and more accurate results of fungal attack along with its prevention can be researched.
- The binder, nanosilica powder and water ratio along with the number of coatings on concrete can be standardized to increase their effectivity to prevent fungal attack on concrete.
- The use of an alternate binder instead of polyethylene gycol can be researched to enhance the effectiveness of nanosilica.
- The effectiveness of other inorganic nanoparticles on prevention of concrete biodeterioration due to fungus can be studied.
- Nanocomposites of silica oxide along with other inorganic nanoparticles could be thoroughly researched for their role in biodeteriorated concrete restoration.

REFERENCES

Adeyemi, A. O., & Gadd, G. M. (2005). Fungal degradation of calcium-, lead-and silicon-bearing minerals. *Biometals*, *18*(3), 269-281

Aldoasri, Mohammad A., et al. "Protecting of Marble Stone Facades of Historic Buildings Using Multifunctional TiO2 Nanocoatings." *Sustainability* 9.11 (2017): 2002.

Aldosari, M. A., Darwish, S. S., Adam, M. A., Elmarzugi, N. A., & Ahmed, S. M. (2019). Using ZnO nanoparticles in fungal inhibition and self-protection of exposed marble columns in historic sites. *Archaeological and Anthropological Sciences*, 1-16.

Allsopp, Dennis, Kenneth J. Seal, and Christine C. Gaylarde. *Introduction to biodeterioration*. Cambridge University Press, (2004) : 1-5, 35-43, 203-223.

Andersen, B., Frisvad, J. C., Søndergaard, I., Rasmussen, I. S., & Larsen, L. S. (2011). Associations between fungal species and water-damaged building materials. *Appl. Environ. Microbiol.*, *77*(12), 4180-4188.

Becerra, J., Zaderenko, A. P., Sayagués, M. J., Ortiz, R., & Ortiz, P. (2018). Synergy achieved in silver-TiO 2 nanocomposites for the inhibition of biofouling on limestone. *Building and Environment*, 141, 80-90.

Bertron, A. (2014). Understanding interactions between cementitious materials and microorganisms: a key to sustainable and safe concrete structures in various contexts. *Materials and Structures*, *47*(11), 1787-1806.

Biswas, Jayant, et al. "Biodeterioration agents: Bacterial and fungal diversity dwelling in or on the pre-historic rock-paints of Kabra-pahad, India." *Iranian Journal of Microbiology* 5.3 (2013): 309.

Brehm, Ulrike, Anna Gorbushina, and Derek Mottershead. "The role of microorganisms and biofilms in the breakdown and dissolution of quartz and glass." *Geobiology: Objectives, Concepts, Perspectives*. Elsevier, 2005. 117-129.

Bruce, A. L. A. N. (1998). Biological control of wood decay. *Forest Products Biotechnology*, 251-266.

Cappitelli, Francesca, et al. "Synthetic consolidants attacked by melanin-producing fungi: Case study of the biodeterioration of Milan (Italy) Cathedral marble treated with acrylics." *Applied and environmental microbiology* 73.1 (2007): 271-277.

Crispim, C. A., & Gaylarde, C. C. (2005). Cyanobacteria and biodeterioration of cultural heritage: a review. *Microbial ecology*, *49*(1), 1-9.

Derrick, M. R., Stulik, D., & Landry, J. M. (2000). *Infrared spectroscopy in conservation science*. Getty Publications.

de Ferri, Lavinia, et al. "Study of silica nanoparticles–polysiloxane hydrophobic treatments for stone-based monument protection." *Journal of Cultural Heritage* 12.4 (2011): 356-363.

Falchi, L., Balliana, E., Izzo, F. C., Agostinetto, L., & Zendri, E. (2013). Distribution of nanosilica dispersions in Lecce stone. *Sciences at Ca'Foscari*, (1| 2013).

Farrukh, M. A. "Antibacterial and Antifungal Activities of Zinc-Sil-icon Oxides Nanocomposite.(2016) Lett Health Biol Sci 1 (1): 1-5." *Lett Health Biol Sci* 1.1 (2016).

Fomina, M., Podgorsky, V. S., Olishevska, S. V., Kadoshnikov, V. M., Pisanska, I. R., Hillier, S., & Gadd, G. M. (2007). Fungal deterioration of barrier concrete used in nuclear waste disposal. *Geomicrobiology Journal*, *24*(7-8), 643-653.

Fomina, M., Hillier, S., Charnock, J. M., Melville, K., Alexander, I. J., & Gadd, G. M. (2005). Role of oxalic acid overexcretion in transformations of toxic metal minerals by Beauveria caledonica. *Appl. Environ. Microbiol.*, *71*(1), 371-381.

Grayston, S. J., & Wainwright, M. (1987). Fungal sulphur oxidation: effect of carbon source and growth stimulation by thiosulphate. *Transactions of the British Mycological Society*, *88*(2), 213-219.

Gesoglu, M., Güneyisi, E., Öz, H. Ö., Yasemin, M. T., & Taha, I. (2015). Durability and shrinkage characteristics of self-compacting concretes containing recycled coarse and/or fine aggregates. *Advances in Materials Science and Engineering*, *2015*.

Givi, A. N., Rashid, S. A., Aziz, F. N. A., & Salleh, M. A. M. (2011). The effects of lime solution on the properties of SiO2 nanoparticles binary blended concrete. *Composites Part B: Engineering*, *42*(3), 562-569.

Gorbushina, Anna A., and Wolfgang E. Krumbein. "Rock dwelling fungal communities: diversity of life styles and colony structure." *Journey to diverse microbial worlds*. Springer, Dordrecht, 2000. 317-334.

Gu, J. D., Ford, T. E., Berke, N. S., & Mitchell, R. (1998). Biodeterioration of concrete by the fungus Fusarium. *International biodeterioration & biodegradation*, *41*(2), 101-109.

Harbulakova, V. O., Estokova, A., Stevulova, N., Luptáková, A., & Foraiova, K. (2013). Current trends in investigation of concrete biodeterioration. *Procedia Engineering*, *65*, 346-351.

Herrera, Liz Karen, et al. "Biodeterioration of peridotite and other constructional materials in a building of the Colombian cultural heritage." *International biodeterioration & biodegradation* 54.2-3 (2004): 135-141.

Hickin, N. (1971). Wood-destroying insects and works of art. *Studies in Conservation*, *16*(sup2), 75-80.

Illescas, Juan F., and Maria J. Mosquera. "Producing surfactant-synthesized nanomaterials in situ on a building substrate, without volatile organic compounds." *ACS applied materials & interfaces* 4.8 (2012): 4259-4269.

Ji, T. (2005). Preliminary study on the water permeability and microstructure of concrete incorporating nano-SiO2. *Cement and concrete Research*, *35*(10), 1943-1947.

Jiang, J., Zheng, Q., Hou, D., Yan, Y., Chen, H., She, W., ... & Sun, W. (2018). Calcite crystallization in the cement system: morphological diversity, growth

mechanism and shape evolution. *Physical Chemistry Chemical Physics*, *20*(20), 14174-14181.

Li, H., Xiao, H. G., Yuan, J., & Ou, J. (2004). Microstructure of cement mortar with nano-particles. *Composites Part B: Engineering*, *35*(2), 185-189.

Luo, J., Chen, X., Crump, J., Zhou, H., Davies, D. G., Zhou, G., ... & Jin, C. (2018). Interactions of fungi with concrete: Significant importance for bio-based self-healing concrete. *Construction and Building Materials*, *164*, 275-285.

Marshman, N. A., & Marshall, K. C. (1981). Bacterial growth on proteins in the presence of clay minerals. *Soil Biology and Biochemistry*, *13*(2), 127-134.

Ogihara, Hitoshi, et al. "Simple method for preparing superhydrophobic paper: spray-deposited hydrophobic silica nanoparticle coatings exhibit high water-repellency and transparency." *Langmuir* 28.10 (2012): 4605-4608.

Pan, X., Shi, Z., Shi, C., Ling, T. C., & Li, N. (2017). A review on concrete surface treatment Part I: Types and mechanisms. *Construction and Building Materials*, *132*, 578-590.

Osman, M. E. S., El-Shaphy, A. A. E. N., & Ayid, M. M. (2017). *Evaluation Of The Inhibitory Effect Of Dimethyl Sulfoxide On Fungal Degradated Archaeological Wood*. International Journal of Conservation Science, 8(3). p431-440.

Rajkowska, Katarzyna, et al. "Assessment of biological colonization of historic buildings in the former Auschwitz II-Birkenau concentration camp." *Annals of microbiology* 64.2 (2014): 799-808.

Rosado, Tânia, et al. "Microorganisms and the integrated conservation-intervention process of the renaissance mural paintings from Casas Pintadas in Évora–Know to act, act to preserve." *Journal of King Saud University-Science* 29.4 (2017): 478-486.

Sanchez-Silva, M., & Rosowsky, D. V. (2008). Biodeterioration of construction materials: state of the art and future challenges. *Journal of Materials in Civil Engineering*, *20*(5), 352-365.

Scevola, D., et al. "Antibacterial activity of nanomolecular silicon dioxide (sio2) combined with silver iones." *Clinical Microbiology & Infection* 18 (2012): 389-390.

Sierra-Fernandez, A., Gomez-Villalba, L. S., Rabanal, M. E., & Fort, R. (2017). New nanomaterials for applications in conservation and restoration of stony materials: A review. *Materiales de Construcción*, *67*(325), 107.

Tiano, P. (2002, April). Biodegradation of cultural heritage: decay mechanisms and control methods. In *Seminar article, New University of Lisbon, Department of Conservation and Restoration* (pp. 7-12).

Warscheid, T., & Braams, J. (2000). Biodeterioration of stone: a review. *International Biodeterioration & Biodegradation*, *46*(4), 343-368.

Wei, S., Jiang, Z., Liu, H., Zhou, D., & Sanchez-Silva, M. (2013). Microbiologically induced deterioration of concrete: a review. *Brazilian Journal of Microbiology*, *44*(4), 1001-1007.

Wheeler, G., & Goins, E. S. (2005). *Alkoxysilanes and the Consolidation of Stone*. Getty Publications, 55-64.

Verrecchia, Eric P. "Fungi and sediments." *Microbial sediments*. Springer, Berlin, Heidelberg, 2000. 68-75.